GREEN SYNTHESIS OF COPPER CHLORIDE NANOPARTICLES USING ONION PEELS FOR THE PHOTOCATALYTIC DEGRADATION OF OIL CONTAMINATED WASTEWATER

BY

Catherine NEHIZENA (Miss)

LSC2104268

DEPARTMENT OF SCIENCE LABORATORY TECHNOLOGY

(CHEMICAL AND PETROLEUM TECHNIQUES)

FACULTY OF LIFE SCIENCES

UNIVERSITY OF BENIN

BENIN CITY

NOVEMBER, 2025.

CERTIFICATION

This is to certify that this project titled *"***SYNTHESIS AND PHOTOCATALYTIC ACTIVITY OF COPPER CHLORIDE NANOPARTICLE FOR DEGRADATION OF CRUDE OIL CONTAMINATED WASTEWATER USING ONION PEEL"** was carried out by **Catherine NEHIZENA,** with matriculation number **LSC2104268**, of the Department of Science Laboratory Technology (chemical and petroleum), Faculty of Life Sciences, University, Benin City, Edo state, Under the supervision of **PROF. J. O. OSARUMWENSE** .

_____ _____

PROF. J. O. OSARUMWENSE

PROJECT SUPERVISOR Date

_____ _____

DR. P.O. ALONGE

PROJECT COORDINATOR Date

_____ _____

PROF. J. O. OSARUMWENSE

HEAD OF DEPARTMENT Date

_____ _____

EXTERNAL EXAMINER Date

DEDICATION

This work is dedicated to God Almighty

ACKNOWLEDGEMENT

When kindness cannot be returned, it should be appreciated. A number of people have helped to make this project research and writing a successful one. So their kindness ought to be appreciated.

My most sincere gratitude goes to my project supervisor Prof J.O. Osarumwense, who took his time in the in-depth supervision of this work and who made sure that this project came to a successful and smooth completion and also for his utmost contribution towards the fulfillment of my dreams of becoming a laboratory scientist. To my late father, whose quiet wisdom and unyielding belief in my dreams lit the path through every challenge, even as you watched from afar. Though you couldn't stay to witness this milestone, your legacy fueled every word on these pages a promise kept, in your honor. I would also like to extend my sincere appreciation to my parents Mr and Mrs Olusoji and my siblings Francess, Joyce and David for their constant encouragement, emotional support, and valuable feedback throughout this project. Their presence in my life has been a source of strength and motivation.

Thank you all for your contributions, support, and guidance. This project would not have been possible without your help.

To Nehikhuere, Mitchelle, Esther, Phillian, Omooba, Mildred, Ruth, Sarah, Annabel, Happy, Praise, Emmanuel, Ada, Kamil, Destiny, Godsent, Elisha and Courage, the ones who stayed up past reason, who passed notes like contraband hope, who turned “I can’t” into “watch me.” You didn’t just stand by me; you carried the weight when my hands shook. This project is yours as much as mine.

I will also like to acknowledge myself for the nights I refused to quit, for the doubts I stared down until they blinked, for every erased line that taught me to begin again. This project is proof that I can show up, messy, tired, determined and still build something that stands.

I am proud of the work, and prouder still of the will that carried it

.

TABLE OF CONTENTS

LIST OF FIGURES

ABSTRACT

This study focused on the green synthesis of copper chloride ($CuCl_2$) nanoparticles using onion peel extract as an eco-friendly reducing and stabilizing agent, and evaluated their efficacy in the photocatalytic degradation of crude oil in contaminated wastewater. The synthesized nanoparticles were characterized Dynamic Light Scattering (DLS),X-ray diffraction (XRD), Thermogravimetric analysis (TGA), Scanning electron microscopy (SEM) and Fourier-Transform Infrared (FTIR) spectroscopy. DLS confirmed the formation of nanoparticles with a primary size of 16.25 nm, XRD determined the crystalline phase of the nanoparticles, TGA measured the thermal stability and decomposition temperature, SEM visualized the particle size, shape, surface texture while FTIR analysis identified functional groups from the onion peel extract, verifying its role in capping and stabilizing the particles. The photocatalytic activity of the nanoparticles was assessed by studying the degradation of total petroleum hydrocarbons (TPH) under sunlight, investigating the effects of catalyst dose, pH, temperature, and initial pollutant concentration. Results demonstrated that the green-synthesized $CuCl_2$ nanoparticles were effective in degrading crude oil components, with optimal performance observed under specific conditions. This indicates that onion peel-mediated $CuCl_2$ nanoparticles present a sustainable, cost-effective, and promising photocatalyst for remediating crude oil-contaminated water, offering a potential solution for environmental cleanup, particularly in oil producing regions like the Niger Delta.

CHAPTER ONE

INTRODUCTION

1.1 BACKGROUND OF STUDY

With roughly 35.2 billion barrels of crude oil reserves, Nigeria ranks twelfth in the world in terms of oil production. Since the discovery of oil in 1956, oil exploration has been going on in the nation. Currently, more than 83% of the nation's overall export profits and 70% of its total revenue come from crude oil. About 606 oil fields (360 onshore and 246 offshore), are used to extract crude oil (Sam *et al*., 2016; Umar *et al*., 2021). Nigeria's oil reserves are located in the Niger Delta, where the majority of oil exploration is conducted. Similar to arable land that supports a diverse range of crops and plants, the Niger Delta is the largest mangrove forest in Africa and a significant global wetland with a wealth of biological diversity. Additionally, according to Ohanmu *et al*. (2019), it boasts more species of freshwater fish than any other habitat in West Africa. The frequent occurrence of oil leak accidents in various locations and at different times throughout the region poses a threat to this rich biodiversity and its swamps and rivers (Sam *et al*., 2016). The Nigerian government and the international oil firms that operate in the region have been called upon on multiple occasions by the impacted communities to clean up the poisoned environment. However, tensions in the areas that produce oil have been exacerbated by the authorities' tardy and insufficient reaction to the pollution issue. In many instances, the complaints have escalated into violent crimes, like as the April 2004 kidnapping and killing of seven military men and employees of the oil business in Delta State (Umar *et al*., 2021; Zabbey *et al*., 2017). Crude oil contamination in Nigeria persists up till date, and remains a problem. The waters in some parts of the Niger delta are in bad shape, due to crude oil contamination.

Fresh water is crucial for the existence of life. About 70 percent of the Earth is covered by water, but a very small portion of this (2.5%) percent is available for different purposes. Uncontrolled population growth in the world has proliferated the industrial revolution, which has caused the pollution of land and water bodies, especially by industrial wastes, which are highly toxic and hardly degradable (Xing *et al*., 2011). Metal oxide composites (e.g Copper chloride ($CuCl_2$)), integrating with carbon materials have attracted a great deal of attention as the potential photo catalysts for environmental treatment. Of recent, metal-oxide based nano-photocatalysts have gained much attention in alleviating waste water conditions due to their properties. Following an oil spill, photo oxidation causes part of the crude oil to be lost. In crude oils with significant water-soluble fractions, this loss from photo oxidation has been found to be predominant (Lehr, 2001). The use of photo catalysts like TiO_2 and $CuCl_2$ may improve this photo oxidation (Dodoo-Arhin *et al*., 2018). As an alternative method for the synthesis of metal and metal oxide nanoparticles, a biological approach to material synthesis has recently been used. This involves environmentally friendly green chemistry-based techniques involving natural materials like plants, bacteria, fungi, seaweed, polysaccharides, biodegradable polymers, plant-derived materials, and algae. As interest in effective green chemistry grows, bio-synthetic methods for creating nanoparticles have drawn a lot of attention due to their simplicity, affordability, cleanliness, and lack of hazardous chemicals, as well as their zero contaminants and byproducts (El-Sayyad *et al*., 2024). Plant extracts have drawn the most interest among these bio-entities because of their unique natural properties, which allow them to stabilize and decrease metal nanoparticles in a single stage of synthesis. Due to their diverse and complex compositions, natural organic phytoconstituent bio-molecules existing in plant extracts such as alkaloids,

flavonoids, saponins, steroids, terpenoids and tannins act as reducing and stabilizing agents (Ishak *et al*., 2019)

1.2 STATEMENT OF THE PROBLEM

The Niger delta region of Nigeria, which hosts the majority of the country's crude reserve, faces severe environmental degradation due to frequent oil spills. These spills contaminate water bodies, threaten biodiversity, and disrupts the livelihood of local communities. Despite repeated calls for remediation, the response from authorities have been slow and inadequate, leading to tensions and violent conflicts like the conflict in the Niger delta (Umar *et al*., 2021). Traditional methods of cleaning up oil-contaminated waste water often involves hazardous chemicals. There is a pressing need for eco-friendly, cost effective and efficient solution to degrade petroleum hydrocarbons in contaminated water.

1.3 AIM

The aim of this work was to synthesize $CuCl_2$ nanoparticle using onion peel as stabilizer for the photocatalytic degradation of oil-contaminated wastewater

1.3.2 The specific objectives of this study are;

- To synthesize $CuCl_2$ nanoparticles using onion peel extract as a green reducing and stabilizing agent
- To characterize the synthesized $CuCl_2$ nanoparticles.
- To evaluate the photocatalytic activity of $CuCl_2$ nanoparticles in degrading crude oil-contaminated waste water**.**

1.4 SCOPE OF THE STUDY

This study was designed to cover the green synthesis of $CuCl_2$ nanoparticles using onion peels, characterize the nano particle using various techniques, and evaluate the photocatalytic activities of the $CuCl_2$ nanoparticles on the degradation of oil contaminated wastewater.

To achieve the scope of the study, the work entails the following:

1. Collection of onion peels from the market, air-dried and ground into powder

2. Extraction of the active components of the onion peels

3. Synthesis of $CuCl_2$ nanoparticles using onion peel extract

4. Characterization of the $CuCl_2$ nanoparticles using various techniques such as XRD, FTIR, TGA, DTA e.t.c

5. Collection of oil contamintaed wastewater

6. Photocalaytic degradation of the wastewater under the sunlight varying contact time, concentration of wastewater, catalyst dose, temperature and pH

1.5 SIGNIFICANCE OF THE STUDY

According to Salem and Ghouniem. (2022), an oil spill is a discrete event that occurs when oil is released over a brief period of time due to negligence, accident, or intentionality. The economy is impacted by oil spills, which primarily occur in marine environments. There are detrimental effects on the economy, nutrition, health, and many other areas when marine life is impacted. For instance, every time there is an oil spill, the standard of living of the fishermen is impacted because it may lead to a decrease in household income. Once more, oil spills devastate the marine environment's shorelines that are used as tourist destinations and recreation areas

(Nyankson, Rodene *et al*., 2016). Therefore, the need to minimize the occurrence and effects of oil spills on the environment cannot be overemphasized. This study focuses on the use of Green synthesis and photocatalytic activity of $CuCl_2$ nanoparticle for degradation of crude oil waste water (Efavi *et al*., 2017).

CHAPTER TWO

LITERATURE REVIEW

2.0 GREEN NANOTECHNOLOGY

The ideal way to lessen the adverse impacts of producing and using nanomaterials is through green nanotechnology, which also reduces the riskiness of nanotechnology (Iavicoli *et al*., 2014). The main benefits of green synthesis are numerous. An important development in materials science and nanotechnology is the creation of engineered nanomaterials. These goods should be taken out of the lab and into the real world. There are thousands of these products on the market, most of which are incorporated into apparel, cosmetics, and daily personal care items. Nearly every industry and production area, including medicine and drug delivery, is anticipated to benefit from the development of contemporary products that consumers require. It is clear that the commercialization of nanomaterials and nano-assisted devices is constantly expanding (Xia *et al*., 2009). Successful disruptive technology commercialization is essential for many human applications and worldwide development, but significant attention is required for the materials' potential, environmental, and health impacts (Wardak *et al*., 2007). It is a well-established fact that the health risks associated with exposure to nanoparticles are not fully understood and must be addressed quickly (Iavicoli *et al*., 2014), and that their production and use are essentially unregulated (Wardak *et al*., 2007), especially in the context of the universe's development.

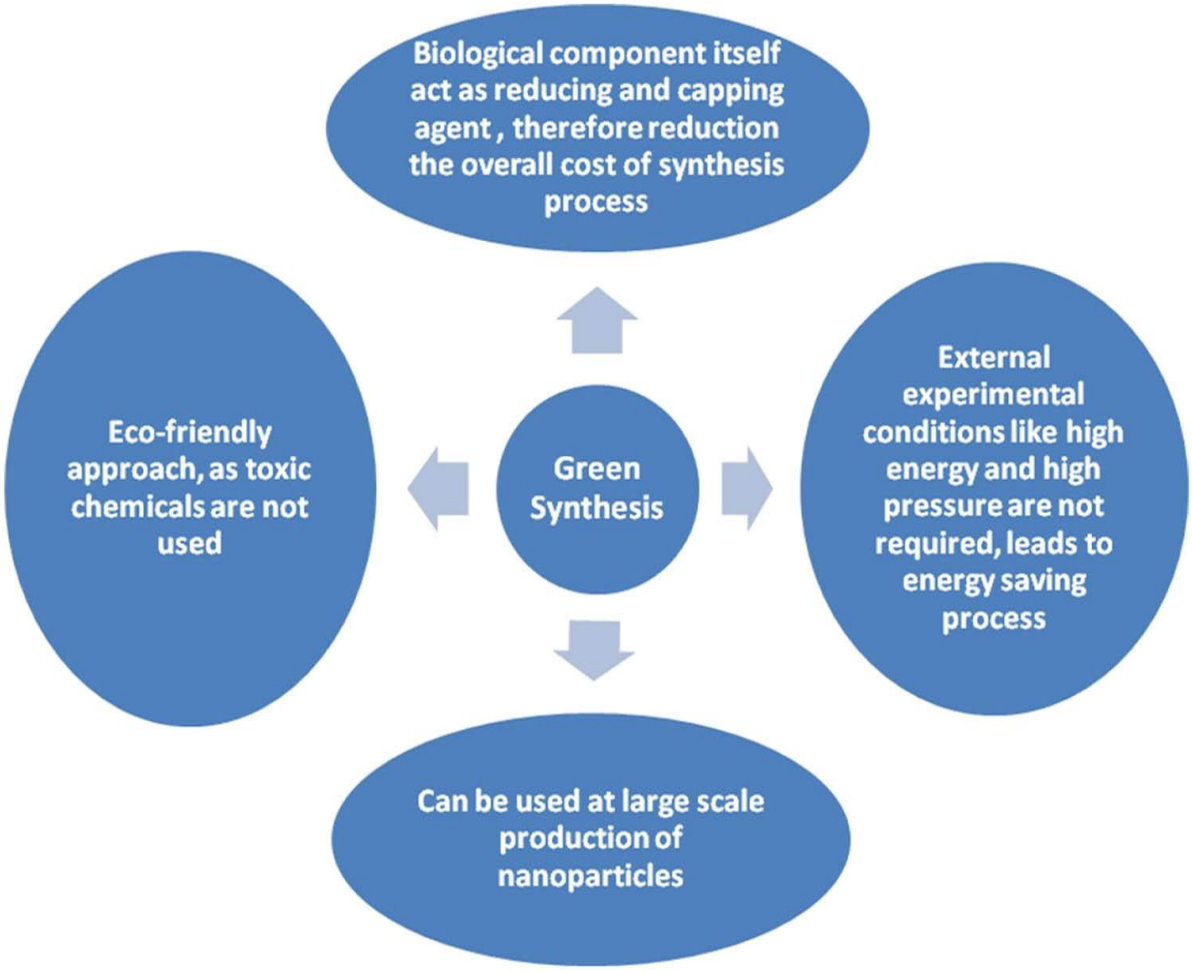

Figure 2.0: Key merits of green synthesis (Singh *et al*., 2018)

2.0.1 GREEN CHEMISTRY

Given that the technology is still in its early stages of development and is expected to be widely used and distributed globally, the use of green chemistry principles in the expansion and enforcement of new materials is all the more significant. New "design principles" for the creation of high rendering nanoscale materials that are safe and environmentally friendly may result from the close relationship between chemical structure and function groups that is unique to nanomaterials and from improving knowledge of "key" information for life cycle evaluation of such methods (Rajender, 2012). The aforementioned plants' chemicals, cells, and organs have been bioengineered to produce novel nanomaterials with demanding, long-term benefits. Green nanotechnology offers us the opportunity to avoid the adverse consequences. By eliminating or reducing pollution, green nanotechnology has an entrepreneurial effect on the design of nanomaterials or products, hence resolving current environmental issues, as seen in Figure 2. In addition to many other factors like size, shape, surface charge, chemical structure, surface area, and coagulation properties of nanoscale distinct materials (Yehia *et al*., 2014), the chemical, physical, and biological properties of nanomaterials are characterized using environmentally friendly techniques like catalytic potential, electrical conductivity (Bonatto and Silva, 2014), optical sensitivity (Quester *et al*., 2013), magnetic behavior (Yehia *et al*., 2014), or biological reactivity.

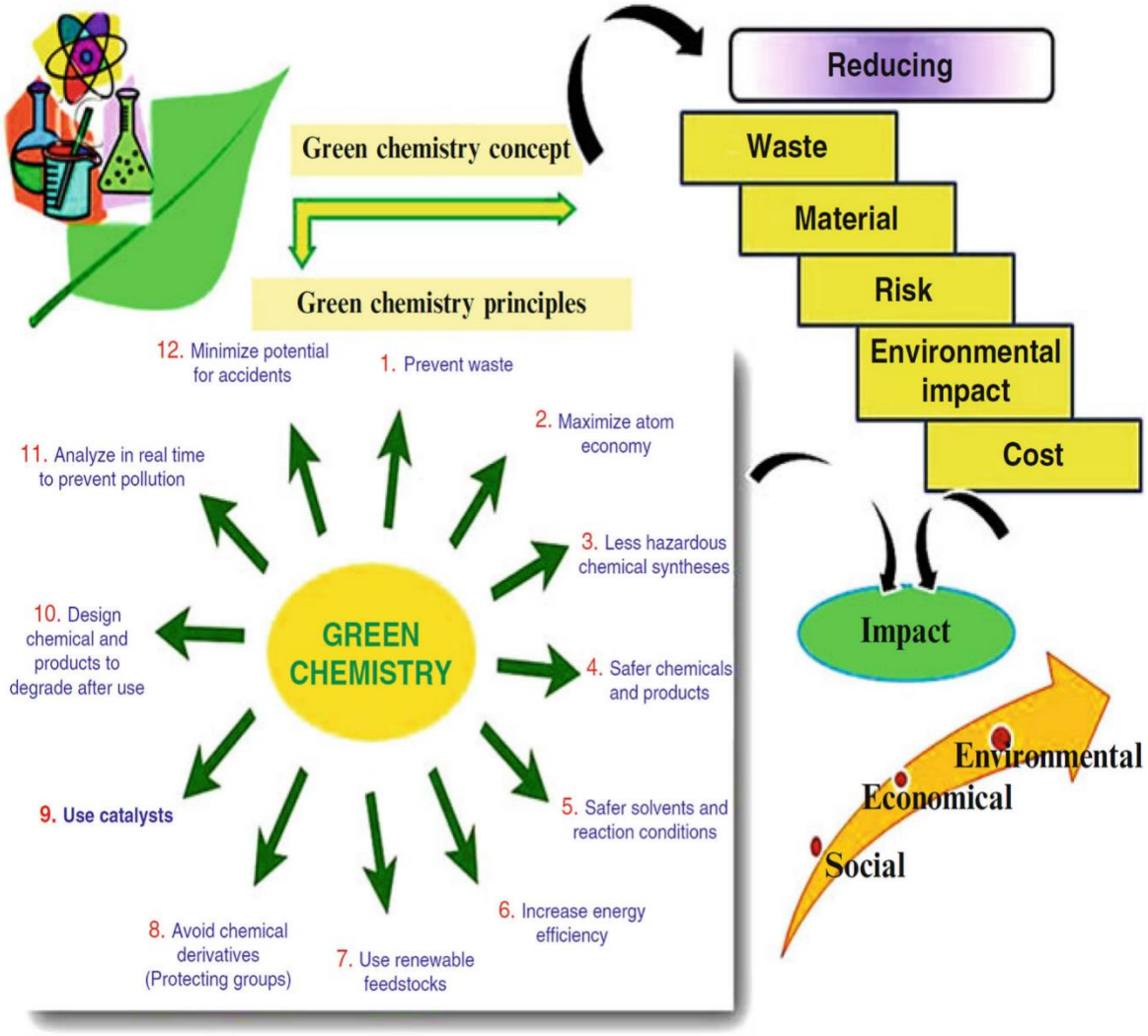

Figure 2.1: Green chemistry (Nath, 2015)

2.0.2 PLANTS AS STABLILIZING AGENTS IN GREEN CHEMISTRY

Living things, which represent the kingdom of the biological system, can be used to create MNPs and MONPs in a green way. In addition to being essential for food and nourishment, living things are also used in green synthesis. Since many plants have a lot of biomass, scientists prioritize using them to carry out the green synthesis of MNPs and MONPs because of their availability of biomass and molecular armament.

Plants primary and secondary metabolites influence their response to stressors (pathogens, herbivores, and climate change) and survival agents (seasonal changes and reproductive methods), which will make plants the primary bioreactors and molecule suppliers for green synthesis. The primary compounds of plants, including amino acids, citric acid (Yehia *et al*., 2014), flavonoids, phenolic compounds, terpenoids (Thakkar *et al*., 2010), heterocyclic compounds, enzymes (Narayanan and Sakthievel, 2011), peptides (Tan *et al*., 2010), polysaccharides (Park *et al*., 2011), saponins (Arunachalam *et al*., 2013), and tannis, are in charge of the metal ion reduction because of the presence of metallic counterparts and the stabilization of the surface of the MNPs and MONPs (Silva *et al*., 2015). The whole organs/tissues or the extracts of the organs/tissues and different parts (e.g., seeds, leaves, barks, roots, and fruits) of the plants are utilized for the green synthesis of MNPs and MONPs and may produce nano-objects with several properties (Kharissova *et al*., 2012), so we deal with each part of the plants discretely for their different concentrations and their unique phytochemical characterization, and this depends on the biotic or abiotic stress type to which a plant perhaps subjected and the needs of each organ.

2.1 GREEN SYNTHESIS OF CuO NANOPARTICLES

Because nanoparticles are used in the scientific, technological, pharmaceutical, and medicinal domains, research on the synthesis and characterization of metallic nanomaterials is a new area of nanotechnology. Nanoparticles have been created using a variety of physical and chemical methods. In addition to being incredibly expensive, the chemical approach of creating nanoparticles has extra risks to the environment and human health. However, biogenic synthesis, which uses plants to produce nanoparticles, is an inexpensive, less expensive, and environmentally beneficial technique. Due to their multifunctional nature, metallic nanoparticles are used in a wide range of fields, including solar power generation, biomedicine, antimicrobials, and catalysis.One A green chemistry technique that forges a close bond between nanosynthesis and natural plant material is the use of plant extracts to create copper and its oxide nanoparticles (Akhtar *et al*., 2013)

According to previous studies (Mubarakali *et al*., 2011; Ravindra *et al*., 2010), copper, gold, and silver nanoparticles shown exceptional antibacterial efficacy against a range of microorganisms that cause disease. Copper nanoparticles (Cu NPs) have become more important in recent years because of their many applications in both industry and health. However, in experiments using Escherichia coli, various nanoparticles, including nickel, silicon oxides, iron oxide, platinum, and gold, have not demonstrated bactericidal effects (Ravindra *et al*., 2010). Cu outperformed Ag in the antibacterial investigation conducted on E. Coli and Bacillus subtilis utilizing Cu and Ag NPs.(6). Cu NPs have wide applications as heat transfer systems (Eastman *et al*., 2012) antimicrobial materials, sensors, and catalysts (Guduru *et al*., 2007). In addition, copper and its compound have been applied as antifungal, antiviral, and molluscicidal agents. The

synthesis of Cu NPs by using extracts of various plants found all over the globe have been reported by many researchers in the past (Kumar *et al*., 2013).

The development of a clean, dependable, biocompatible, affordable, and nontoxic green technology for synthesizing nanoparticles is crucial. Because plants contain a wide variety of bioactive chemicals, many plant parts or entire plants have been employed for the environmentally friendly synthesis of Cu NPs (Mondal *et al*., 2011). For this purpose, plant extracts from *Nerium oleander* (Gopinath *et al*., 2014), *Punica granatum*, Aegle marmelos, and *Ocimum sanctum*, as well as *Zingiber officinale*, have been effectively used (Kulkarni *et al*., 2014).

2.1.1 GREEN SYNTHESIS OF Cu and CuO NANOPARTICLES

Plants consists of large number of biologically active compounds and hence, most of the plants have proven record for their anthelmintic, antitumor, antimutagenic, antibacterial and fungicidal properties. The synthesis of metallic NPs involves simple mixing of metal solution with extract of plant. Nanoparticles are produced in the medium due to reduction of metal ions. The most popular precursor copper salts, cupric acetate (monohydrate) ((CH3COO)2Cu·H2O), copper chloride di-hydrate (CuCl2. 2H2O) (Rajesh *et al*., 2018), and copper sulfate pentahydrate (CuSO4.5H2O), can be used to synthesize Cu NPs, according to numerous previous studies (Nagajyothi *et al*., 2017). The nature and characteristics of synthetic Cu NPs and CuO NPs are influenced by a number of variables, including temperature, pH, and concentration.

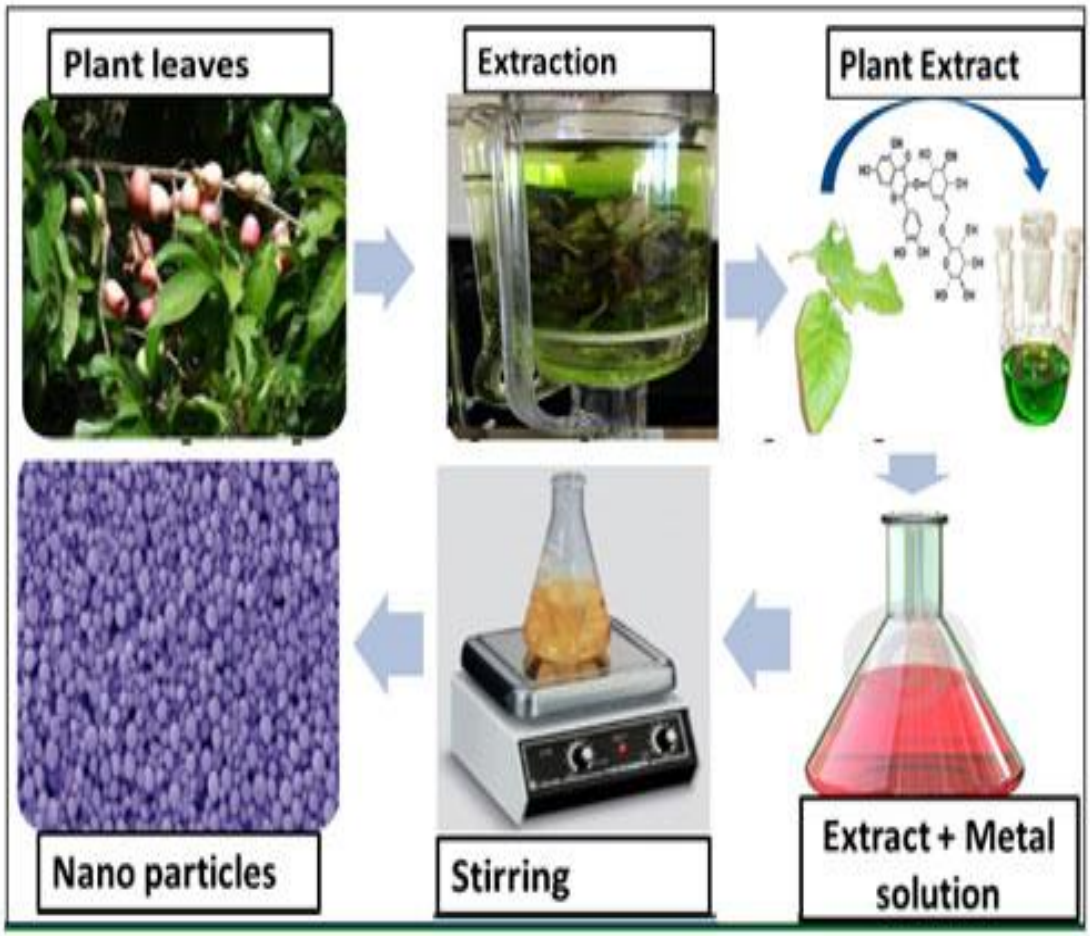

Figure 2.1: Green synthesis of CuO nanoparticles (Ananda Murthy *et al*., 2018)

The transformation of copper ions into stable copper nanoparticles has been linked to the bioactive compounds present in the leaf extract of *Azadirachta indica* (Nagar and Devra, 2018). In this investigation, it was observed that the rate of nanoparticle formation increased proportionally with the concentration of leaf broth used. The optimal parameters for synthesis were identified as [CuCl2] = 7.5×10^{-3} M, pH 6.6, and a reaction temperature of 85°C. Similarly, the green synthesis of copper nanoparticles stabilized with *Tinospora cordifolia* (Cu NPs@Tc) has also been documented (Sharma *et al*., 2018). Successful biosynthesis of Cu nanoparticles has been achieved using extracts derived from different plant sources, including juice of *Citrus medica Linn.* (Idilimbu) (Shende *et al*., 2015), *Ziziphus spina-christi* (L.) Willd, root and leaf extracts of *Asparagus adscendens* Roxb (Thakur *et al*., 2018), leaves of *Eclipta prostrata* (Chung *et al*., 2017), *Ginkgo biloba* Linn (Nasrollahzadeh and Sajadi, 2015), *Plantago asiatica* leaf *Thymus vulgaris* L (Issaabadi *et al*., 2017), black tea leaves (Asif *et al*., 2018), *Terminalia catappa* leaf, among several others (Vishveshar *et al*., 2018)..

2.2.2 CHARACTERIZATION OF Cu AND CuO NANOPARTICLES

The characterization of biogenetically synthesized Cu and CuO nanoparticles has been carried out using several analytical techniques, including UV–Visible spectroscopy, XRD, EDS, DLS, SEM, TEM, FTIR, HRTEM, particle analyzers, and surface plasmon resonance. UV - Vis absorption spectroscopy was particularly employed to monitor the color change observed in copper nanoparticles synthesized with *Ziziphus spina-christi* leaves, (Khani *et al*., 2018), which is likely attributed to surface plasmon vibrations. The surface plasmon resonance bands of Cu-NPs produced by different plant extracts generally ranged from 191 nm to 721 nm.

XRD analysis confirmed the crystalline nature of the nanoparticles, with intense peaks detected for Cu NPs synthesized from citron juice (Shende *et al*., 2015), and crystalline CuO NPs obtained using *Aloe vera* extract (Muthulakshmi *et al*., 2017). FT IR spectral studies provided insights into the functional groups of biomolecules involved in the synthesis. Prominent IR peaks were recorded at 3,333 cm^{-1} for hydroxyl groups (H-bonded OH stretch), 2,917 cm^{-1} for methylene C-H asymmetric/symmetric stretches, and 1,615 cm^{-1} corresponding to aromatic ring vibrations.27 Additional peaks near 3400, 1650, 1595, 1400, and 1100 cm^{-1} were associated with –OH, C=O, C=C, C–OH, and C–H bonds, respectively.28 Characteristic cellulose bands appeared at 3304 cm^{-1}, 2891 cm^{-1}, 1664 cm^{-1}, and 1011 cm^{-1}, reflecting vibrations of –OH, CH_2, H_2O, and C–OH groups (Muthulakshmi *et al*., 2017). Bands at 610, 499, and 415 cm^{-1} confirmed Cu–O vibrations, indicating monoclinic CuO phases in nanoparticles synthesized from *Aloe barbadensis Miller* extract. An additional band around 800 cm^{-1} corresponded to C–H out-of-plane bending, suggesting the adsorption of phenolic compounds onto CuO nanoparticles (Sorbium *et al*., 2018).

Electron microscopy was applied for both morphological assessment and internal structural analysis of biogenic Cu and CuO nanoparticles. Elemental composition was determined using EDS. FE SEM imaging revealed that biogenic Cu NPs were generally uniform and spherical, with particle sizes ranging from 20 nm to 500 nm. TEM micrographs supported this observation, showing spherical nanoparticles with minimal aggregation. DLS analysis further confirmed particle size distribution, with Cu NPs synthesized from *Azadirachta indica* leaves averaging around 50 nm. (Nagar and Devra, 2018) TEM studies also verified spherical morphology and narrow size distribution, (Nasrollahzadeh and Sajadi, 2015) while *Aloe vera* biomolecules acting

as stabilizers and capping agents increased particle size up to 30 nm without altering the spherical shape.

FESEM results for CuO NPs also showed spherical forms ranging between 20 nm and 300 nm. Nanoparticles produced from oak fruit extract averaged about 34 nm, (Sorbium *et al*., 2018) though some exhibited aggregation, increasing the mean size up to 300 nm. (Vishveshvar *et al*., 2018) HRTEM analysis of CuO NPs synthesized with *Syzygium alternifolium* fruit extract recorded particles as small as 2 nm. CuO NPs prepared from *Ferulago angulata* extract (Shayegan *et al*., 2017) displayed sheet-like shell structures, while well-dispersed, nearly spherical particles sized 15–25 nm were also achieved without aggregation. TEM examination of CuO NPs synthesized using *B. tomentosa* leaf extract (Sharmila *et al*., 2018) revealed spherical morphology with sizes ranging from 22 to 40 nm.

2.2.2 APPLICATION OF Cu AND CuO NANOPARTICLES

Copper (Cu) and copper oxide (CuO) nanoparticles possess diverse functionalities, making them highly valuable in a wide range of applications such as antimicrobial and antiviral activity, catalytic and photocatalytic degradation, anticancer activity, biofilm inhibition, nitrate removal, action against human pathogens, photoluminescence, and organic dye degradation, among others.

Cu NPs have shown strong antibacterial effects against *Bacillus* species and notable antifungal activity against *Penicillium* species. (Rajesh *et al*., 2018). They also exhibited higher inhibitory activity on *Escherichia coli* compared to *Klebsiella pneumoniae*, *Pseudomonas aeruginosa*, *Propionibacterium acnes*, and *Salmonella typhi*. In addition, *Fusarium culmorum* was identified as a particularly sensitive plant pathogenic fungus (Thakur *et al*., 2018). Beyond antimicrobial

activity, Cu NPs have also been employed in antioxidant and cytotoxic studies (Chung *et al*., 2017). Green synthesized Cu NPs using *Ginkgo biloba* leaf extract (Nasrollahzadeh and Sajadi, 2015)), were applied as catalysts in the Huisgen [3 + 2] cycloaddition reaction, while those derived from *Ziziphus spina-christi* fruits served as efficient nanoadsorbents for removing Crystal Violet from aqueous solutions (Khani *et al*., 2018)).

CuO nanoparticles prepared using oak fruit hull extract were effective in degrading Basic Violet 3 dye in water (Sorbium *et al*., 2018). Similarly, *Rheum palmatum* L. extract was used to synthesize CuO NPs that acted as efficient catalysts for the degradation of 4-nitrophenol, methylene blue, rhodamine B, and Congo red (Herrera and Reyes, 2017). Their catalytic efficiency is largely attributed to the high surface-to-volume ratio and abundance of active sites. Additionally, CuO NPs have functioned as photocatalysts (Aminuzzaman *et al*., 2017), for Congo red degradation and as nanocatalysts in arylation reactions (Manjari *et al*., 2017).

Further studies reported that CuO NPs synthesized from aqueous extracts of *Anthemis nobilis* flowers, (Nasrollahzadeh *et al*., 2015) *Thymus vulgaris* leaves, and *Euphorbia esula* L. displayed catalytic efficiency in aldehyde-amine-alkyne (A3) coupling reactions and Ullmann-type coupling reactions. CuO NPs prepared from *Saraca indica* leaves exhibited notable photoluminescent properties. (Prasad *et al*., 2017) Biogenically synthesized CuO NPs using *Aloe vera* leaf extract demonstrated antimicrobial activity against fish bacterial pathogens. (Kumar *et al*., 2015)

Additionally, Cu nanoparticles and nanobiocomposites produced from both plant and animal sources have shown promising potential in electronic device applications. For example, Cu NPs synthesized with pomegranate (*Punica granatum*) peel extract68 displayed significant

antibacterial activity against pathogenic microorganisms. Overall, a wide variety of plant extracts have been explored for the eco-friendly synthesis of Cu and CuO nanoparticles, with applications spanning antimicrobial (including urinary tract infections), catalytic, photocatalytic, antioxidant, and dye degradation processes (Shaikh and Lettre, 2016; Delma *et al*., 2016; Sivaraj *et al*., 2014; Nazar *et al*., 2018)).

2.3 PHOTOCATALYTIC DEGRADATION OF HYDROCARBONS

An oil spill refers to a distinct incident in which oil is released either accidentally, through negligence, or deliberately within a short time frame (Etkin, 2001). These spills, which commonly occur in marine environments, trigger widespread socio-economic impacts. When aquatic life is disrupted, consequences extend to food security, health, and income generation. For example, the livelihood of fishing communities is directly threatened since oil spills reduce household earnings. Likewise, coastlines that function as recreational and tourist attractions are damaged, while some marshlands may be permanently destroyed (Nyankson *et al*., 2016). Ultimately, such negative outcomes hinder the full economic benefits of the oil industry.

Thus, minimizing both the frequency and the impact of oil spills is of critical importance. Several remediation techniques are widely used, including chemical dispersants, mechanical containment and recovery, in-situ burning, application of biological agents to enhance degradation, and the use of sorbent materials. Although these strategies have significantly reduced environmental damage, many of them face persistent limitations. For instance, chemical dispersants are costly and toxic, posing risks to ecosystems and cleanup personnel (Nyankson *et al*., 2016). To address these concerns, biodegradable and eco-friendly dispersants derived from soybean lecithin have been developed (Efavi *et al*., 2017; Nyankson *et al*., 2015; Nyankson *et al*., 2016). Additionally, other researchers have explored the use of naturally occurring halloysite

nanotubes and crude oil–soluble paraffins in dispersant formulations (Nyankson, 2015; Nyankson *et al*., 2014; Nyankson *et al*., 2015; Owoseni *et al*., 2014, 2016). The function of chemical dispersants lies in lowering the interfacial tension between oil and water. When sufficient energy is applied, the oil slick disperses into smaller droplets that diffuse both vertically and horizontally within the water column, where marine bacteria can then degrade them. However, research conducted years after the Gulf of Mexico oil spill revealed that water-soluble fractions of the oil persisted (Ziervogel *et al*., 2012). In contrast, paraffins are known to undergo relatively faster biodegradation. Since different fractions of crude oil respond uniquely to degradation, the development of a strategy capable of efficiently targeting all fractions is essential.

In addition to microbial degradation, some crude oil fractions are lost through photooxidation, especially those rich in water-soluble components. Photooxidation can be enhanced with photocatalysts such as TiO_2 (Dodoo-Arhin *et al*., 2018). The present study investigates how various crude oil fractions respond to photocatalysis, providing insight into whether photocatalysis could serve as a standalone remediation technique or be integrated with existing approaches for improved efficiency. Photocatalysis involves the acceleration of a photochemical reaction in the presence of a catalyst. When a photocatalyst (e.g., TiO_2) is irradiated with light of energy equal to or greater than its band gap, electrons transition from the valence band to the conduction band, generating electron–hole pairs. The valence band holes act as strong oxidizing agents, while conduction band electrons serve as strong reducing agents. These reactive sites interact with water and dissolved oxygen to produce reactive oxygen species (ROS), which in turn degrade pollutants into harmless byproducts. Photocatalysis has proven effective in breaking down water-soluble pollutants such as dyes, pesticides, and pharmaceuticals (Nyankson *et al*.,

2019a; Nyankson *et al*., 2019b; Nyankson and Kumar, 2019). Given the complex organic composition of crude oil, it is hypothesized that photocatalysis could effectively degrade its multiple fractions.

A range of photocatalysts, including Ag_3PO_4, ZnO, SnO_2, ZrO_2, TiO_2, and CuO, have demonstrated efficacy in pollutant degradation (Agbe *et al*., 2019). Among these, TiO_2 is particularly advantageous due to its high chemical and thermal stability, adjustable band gap, and wide availability (Ajaj, 2015; Chong *et al*., 2010; Fujishima and Zhang, 2006; Fujishima *et al*., 2007; Huang *et al*., 2016 Nasiri *et al*., 2018; Santos *et al*., 2012). The photochemical degradation of crude oil polycyclic aromatic hydrocarbons using TiO_2 has been reported and modeled (Plata *et al*., 2008). However, the wide band gap of TiO_2 (~3.2 eV) restricts its absorption to the UV spectrum, which represents only about 4% of solar radiation reaching the Earth's surface (Martin *et al*., 2015; Murphy *et al*., 2006). This limitation reduces its practical effectiveness.

To overcome this, TiO_2 has been modified through doping or heterojunction formation, allowing absorption in both UV and visible light regions. Such modifications improve photoabsorption and pollutant degradation efficiency (Ajaj, 2015; Huang *et al*., 2016). TiO_2 performance has also been enhanced by coupling with semiconductors such as Ag_3PO_4 (Lu *et al*., 2015) or by decoration with Ag (Coto *et al*., 2017) and Fe (Fàbrega *et al*., 2010). Among these, Fe is a preferred modifier due to its unique half-filled electronic configuration and relatively lower cost compared to Ag. This configuration not only narrows the band gap but also reduces electron–hole recombination, thereby enhancing photocatalytic efficiency (Meng *et al*., 2013).

CHAPTER THREE

MATERIALS AND METHODLOGY

3.1 MATERIALS

3.1.1 APPARATUS, EQUIPMENT AND INSTRUMENT

Measuring cylinder

Conical flask

Beaker

Crucible

Magnetic stirrer

Hot plate

Funnel

Mesh

Volumetric flask

Aluminium foil paper

Paper tape

Round bottom flask

Separating funnel

Retort stand

Oven

Muffle furnance

Weighing balance

Thermometer

pH meter

Centrifuge

Spectrophotonmeter

X-ray diffractometer

FTIR spectrophotometer

Dynamic light scattering machine

Thermogravimetric analyzer 4000

Scanning electron microscope.

3.1.2 SOLVENT AND REAGENT

Distilled water

Sodium hydroxide

N-Hexane

Copper chloride

Onion peel extract

3.2 SAMPLE COLLECTION

Onion peel was collected from ring road area of Benin City in august 2025. The onion peel was

identified and authenticated by Prof. Akinibosun of the department of plant biology and biotechnoogy, University of Benin. The sample consist of onion peel which was air dried and then into powder using a mechanical grinder and stored in a clean container.

3.3 EXTRACTION

Onion peel extract was prepared by soaking 30g of the dry powdered onion peel in 600ml of distilled water at 70℃ for 2 hours (for thorough extraction). The extract was then filtered through a mesh cloth, poured into a container and stored in a freezer for further use

3.4 SYNTHESIS OF COPPER NANOPARTICLE

In a 1000ml conical flask 1.705ml of $CuCl_2$ was mixed with a 100ml of onion peel extract prepared above and stirred at room temperature for 2hours .After 2hours drops saturated NaOH was added till it got to a pH of 10. The color of the mixture gradually changed from a blue to a bluish green indicating the formation of $CuCl_2$ nanoparticles. The resulting precipitate was obtained by allowing it to settle for hours, then washed with distilled water till a neutral pH is obtained. The precipitate was then centrifuged at 4000rpm for 10minutes ,oven dried at 100℃ for 1hour, casined in a muffle furnace at 450℃ for 2hours and then collected for further characterization.

3.5 PHOTOCATALYTIC DEGRADATION STUDY

The photocatalytic degradation was carried out following the method of J. Saien and H. Nejati, 2007

3.5.1 Effect of catalyst dose

A 100ml of 1000ppm solution of petroleum contaminated waste was placed in a 250ml

erlenmeyer flask thereafter 0.05g of catalyst dose was placed in it and allowed to stay under the sun for 5 hours with shaking intermittently this was repeated for 0.04g ,0.03g, 0.02g and 0.01g. The mixture was centrifuged. 50mL of the supernatant solution was extracted with 10mL of N-hexane and the total hydrocarbon was determined using a UV-Visible spectrophotometer at 460nm (Ademoroti,1996)

3.5.2 Effect of contact time

A 100mL of 1000ppm solution of petroleum contaminated waste was placed in a 250ml erlenmeyer flask thereafter 0.05g of catalyst dose was place in it and allowed to stay under the sun for 1 hour with shaking intermittently this was repeated for 2hours,3hours, 4hours and 5hours. The mixture was centrifuged. 50mL of the supernatant solution was extracted with 10mL of N-hexane and the total hydrocarbon was determined using a UV-Visible spectrophotometer at 460nm (Ademoroti,1996).

3.5.3 Effect of concentration

A 100mL of 200ppm solution of petroleum contaminated waste was placed in a 250mL erlenmeyer flask thereafter 0.05g of catalyst dose was place in it and allowed to stay under the sun for 5hours with shaking intermittently this was repeated for 400ppm, 600ppm, 800ppm and 1000pm. The mixture was centrifuged. 50mL of the supernatant solution was extracted with 10mL of N-hexane and the total hydrocarbon was determined using a UV-Visible spectrophotometer at 460nm (Ademoroti,1996).

3.5.4 Effect of temperature

A 50mL of 1000ppm solution of petroleum contaminated waste was placed in a 250mL erlenmeyer flask thereafter 0.025g of catalyst dose was place in it and allowed to stay under sun in a water bath at 20℃ for 5hours with shaking intermittently this was repeated for 25℃ , 30℃,

35℃ and 40℃ . The mixture was centrifuged. 50mL of the supernatant solution was extracted with 10mL of N-hexane and the total hydrocarbon was determined using a UV-Visible spectrophotometer at 460nm (Ademoroti,1996).

3.5.5 Effect of pH

The optimum pH study was done by adjusting the pH of the solution with 0.1M solution of NaOH for a basic pH and 0.1M solution of HCl for an acidic pH

A 100mL of the prepared solution of acidic petroleum contaminated waste with a pH of 2 was placed in a 250mL erlenmeyer flask thereafter 0.05g of catalyst dose was place in it and allowed to stay under sun for 5hours with shaking intermittentlyon a water bath at 40℃ this was repeated for pH 4,pH 6, pH 8 and pH 10 . The mixture was centrifuged. 50mL of the supernatant solution was extracted with 10mL of N-hexane and the total hydrocarbon was determined using a UV-Visible spectrophotometer at 460nm (Ademoroti,1996).

3.6 CHARACTERIZATION

3.6.1 X-Ray Diffraction (XRD)

X-Ray Diffraction analysis was employed to determine the crystalline phase, crystal structure, and average crystallite size of the synthesized nanoparticles. The powdered nanoparticle sample, obtained after calcination, was evenly packed into a standard sample holder. XRD analysis was performed using an X-ray diffractometer (e.g., Bruker D8 Advance) equipped with a Cu Kα radiation source ($\lambda = 1.5406$ Å). The data were collected in the 2θ range of 10° to 80° with a step size of 0.02° and a counting time of 1 second per step. The resulting diffraction pattern was compared with standard reference patterns from the International Centre for Diffraction Data (ICDD) database for phase identification of $CuCl_2$ or its potential transformation products (e.g.,

CuO or Cu_2O). The average crystallite size (D) was calculated from the full width at half maximum (FWHM, β) of the most intense diffraction peak using the Debye-Scherrer equation.

3.6.2 Thermogravimetric Analysis (TGA) and Differential Thermal Analysis (DTA)

TGA and DTA were used to investigate the thermal stability, decomposition profile, and phase transformations of the nanoparticles, particularly important given the use of a biological capping agent (onion peel extract). A small quantity (approximately 5-10 mg) of the synthesized nanoparticle powder was loaded into a platinum crucible. The analysis was performed using a simultaneous TGA/DTA thermal analyzer 4000 by Perkin Elmer Netherlands The sample was heated from room temperature to 800 °C at a constant heating rate of 10 °C per minute under a controlled nitrogen or air atmosphere with a flow rate of 100 mL/min. The TGA curve recorded the mass loss as a function of temperature, indicating events such as moisture evaporation, decomposition of the organic capping agents from the onion peel extract, and any phase changes. The corresponding DTA curve identified endothermic or exothermic peaks associated with these thermal events, such as crystallization or decomposition.

3.6.3 Fourier-Transform Infrared Spectroscopy (FTIR)

FTIR spectroscopy was utilized to identify the functional groups present on the surface of the nanoparticles and to confirm the role of onion peel extract as a reducing and stabilizing agent. Approximately 1-2 mg of the dried nanoparticle powder was thoroughly mixed with 100 mg of anhydrous potassium bromide (KBr) and pressed into a transparent pellet using a hydraulic press under a pressure of 7-10 tons. The FTIR spectrum was recorded in transmission mode using an FTIR spectrometer (PerkinElmer Spectrum Two) over a wavenumber range of 4000 to 400 cm^{-1}

with a resolution of 4 cm^{-1}. A background spectrum of a pure KBr pellet was collected and automatically subtracted from the sample spectrum. The characteristic absorption peaks were assigned to specific molecular vibrations (e.g., O-H stretch, C=O stretch, C-O stretch) of the phytochemicals from the onion peel extract, confirming their presence on the nanoparticle surface.

3.6.4 Dynamic Light Scattering (DLS) and Zeta Potential

DLS and Zeta Potential measurements were performed to determine the hydrodynamic diameter size distribution of the nanoparticles in suspension and their surface charge, which are critical indicators of colloidal stability. The nanoparticle powder was dispersed in deionized water to a final concentration of approximately 0.1 mg/mL. The suspension was subjected to ultrasonication in a water bath for 30 minutes to ensure a mono-disperse state and break down loose aggregates. Subsequently, 1 mL of the suspension was transferred into a disposable polystyrene cuvette (for DLS) and a folded capillary cell (for zeta potential). Measurements were carried out using a Zetasizer instrument (Malvern Panalytical Zetasizer Nano ZS) at a fixed temperature of 25°C. The hydrodynamic diameter and polydispersity index (PDI) were obtained from the DLS measurement. The zeta potential was determined via Laser Doppler Velocimetry. The reported values represent the mean of three consecutive measurements.

3.6.5 Scanning Electron Microscopy (SEM)

Scanning Electron Microscopy was utilized to investigate the surface morphology, primary particle size, and agglomeration state of the nanoparticles. A dilute suspension of the nanoparticles in deionized water was prepared via ultrasonication for 15 minutes. A single drop of the suspension was deposited onto a clean aluminum stub and allowed to air-dry under

ambient conditions. The dried sample was subsequently sputter-coated with a thin layer (approximately 10-15 nm) of gold to enhance surface conductivity. The coated sample was then transferred to the chamber of the SEM. Imaging was performed at an accelerating voltage of 15-20 kV under high vacuum mode. Multiple micrographs were captured at various magnifications (e.g 50,000x to 100,000x) from different regions of the sample to ensure representative analysis.

CHAPTER FOUR

RESULTS

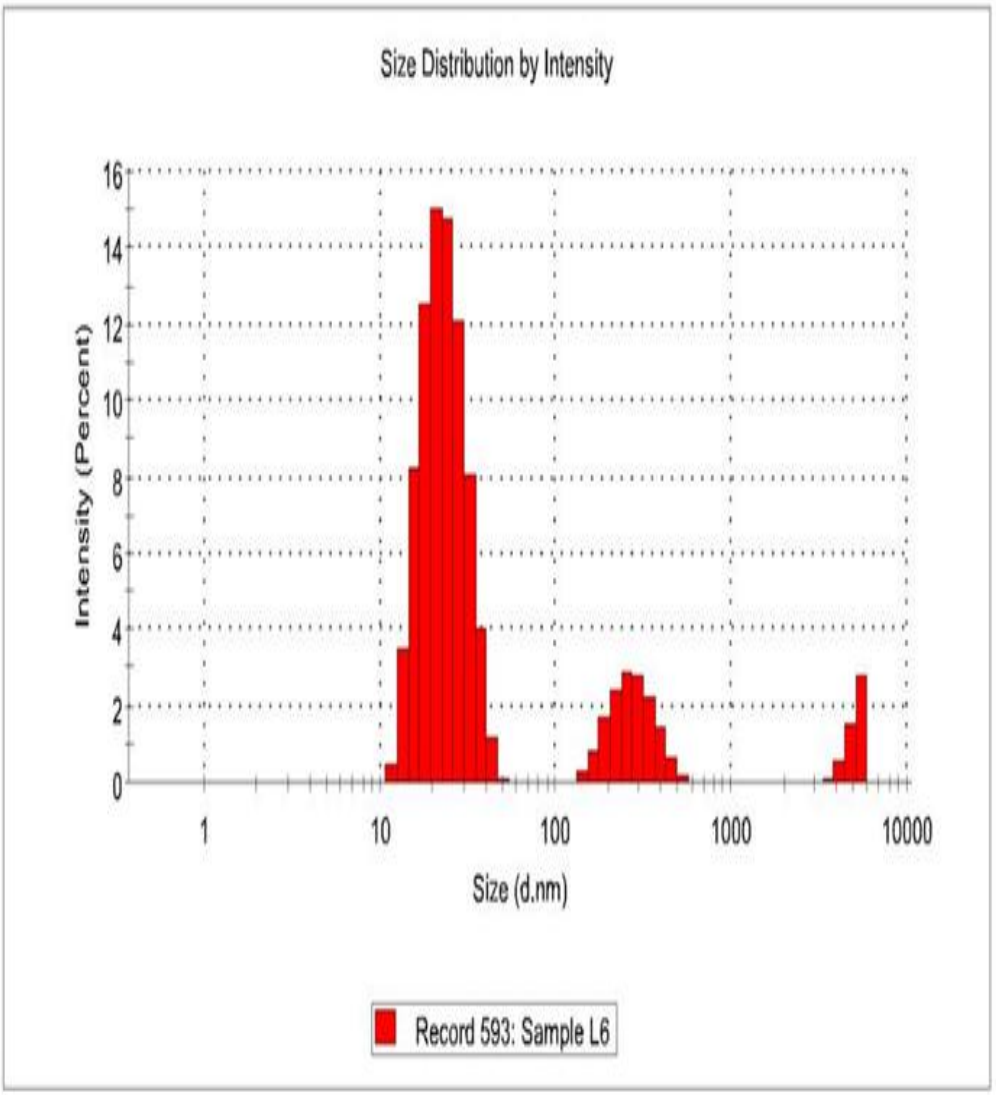

Figure 4.1: Size distribution by intensity

Figure 4.1: Size Distribution Report by Intensity: This Dynamic Light Scattering (DLS) report, presenting data based on light scattering intensity, established a Z-Average hydrodynamic diameter of 45.82 nm for the copper chloride nanoparticles (NPs), with a respectable Polydispersity Index (PDI) of 0.193. This low PDI initially suggests a relatively monodisperse sample. However, the intensity distribution graph reveals a tri-modal profile, which explains the complexity; the primary population, accounting for the largest share of scattered light, is centered at 22.74 nm (78.9 % intensity), while two minor peaks are observed at 275.9 nm (4.9%) and a significantly large size of 5154 nm (approx 5.15 mum, 4.9%). These larger peaks, despite their low percentage, are indicative of the presence of some large aggregates within the suspension.

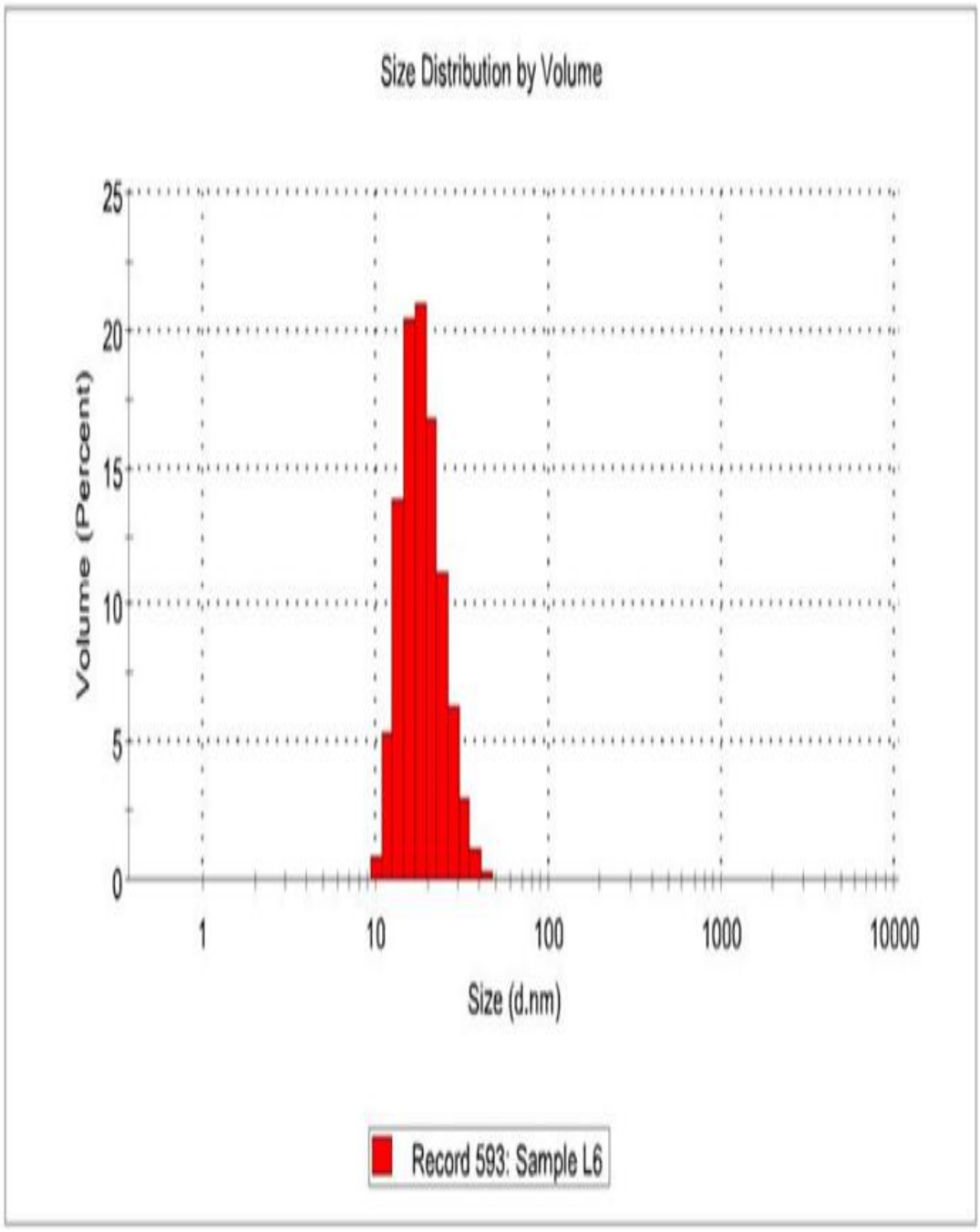

Figure 4.2: Size distribution by volume

Figure 4.2 - Size distribution by volume: The Volume Distribution report provides a view of the particle size based on the volume of the material, which is often considered a better measure of the material quantity than intensity. This analysis reinforces the finding that the vast majority of the synthesized material is small, with the main peak centered at 19.4 nm and constituting 98.7%$of the total particle volume. This result strongly validates the efficiency of the green synthesis in producing tiny nanoparticles. The Z-Average and PDI remain the same as the intensity report, 45.82 nm and 0.193, respectively.

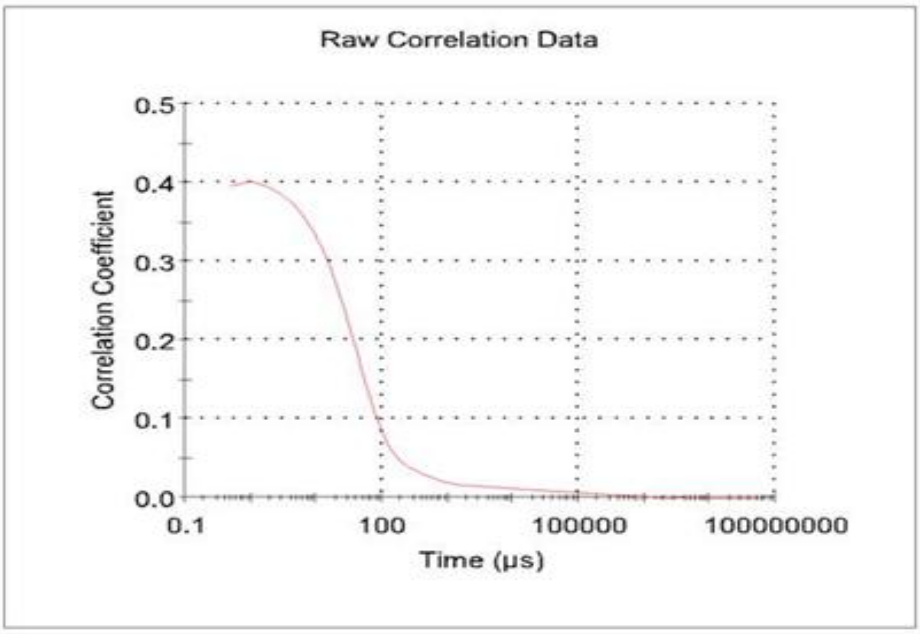

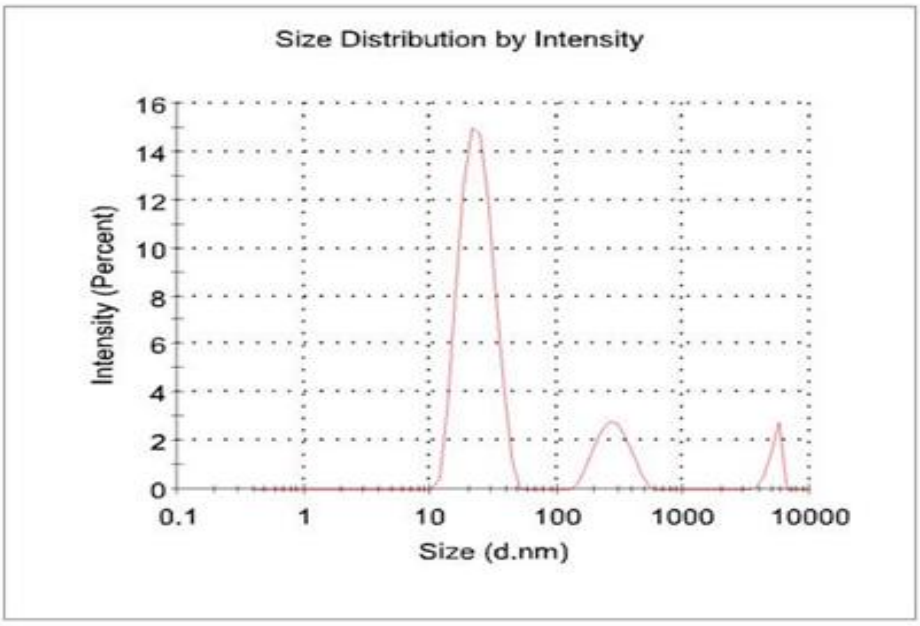

Figure 4.3: Size quality

Figure 4.3: Size Quality Report: This critical report flags a caution regarding the reliability of the DLS calculation, explicitly stating that the "RESULT DOES NOT MEET QUALITY CRITERIA". The primary reason given is a high cumulant fit error, which means the mathematical model used to calculate the Z-Average and PDI did not accurately fit the raw correlation data. This warning suggests that a single average size (the Z-Average) is an insufficient representation of the sample due to its heterogeneity (the presence of both small NPs and large aggregates), and recommends relying instead on the distribution analysis

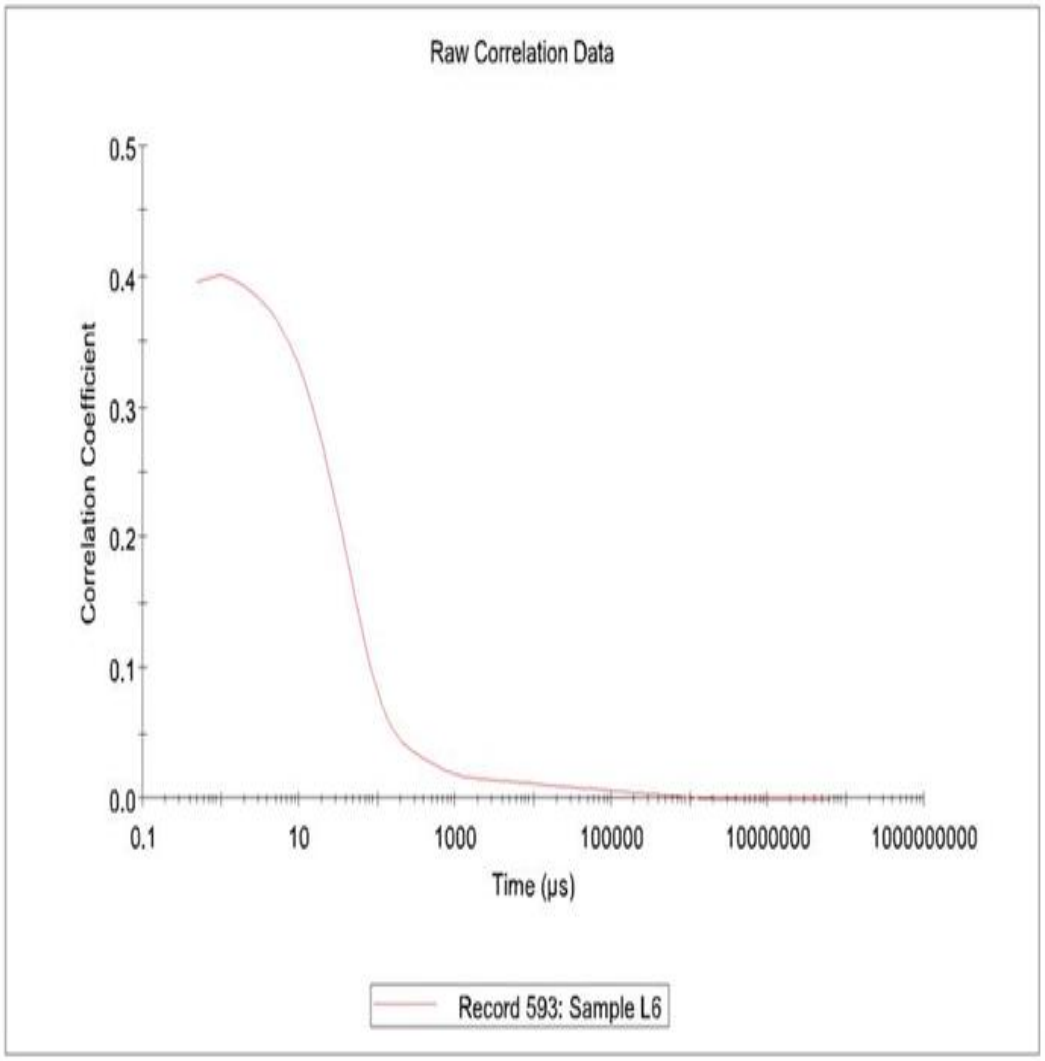

Figure 4.4: Correlation coefficient

Figure 4.4: The Correllogram displays the fundamental DLS data as the Raw Correlation Coefficient plotted against time (in microseconds, μs). The curve represents how quickly the scattered light intensity from the particles decorrelates due to Brownian motion. The initial steep decay of the correlation function, occurring predominantly between 10 and 100 μs, is characteristic of the fast movement of small nanoparticles.

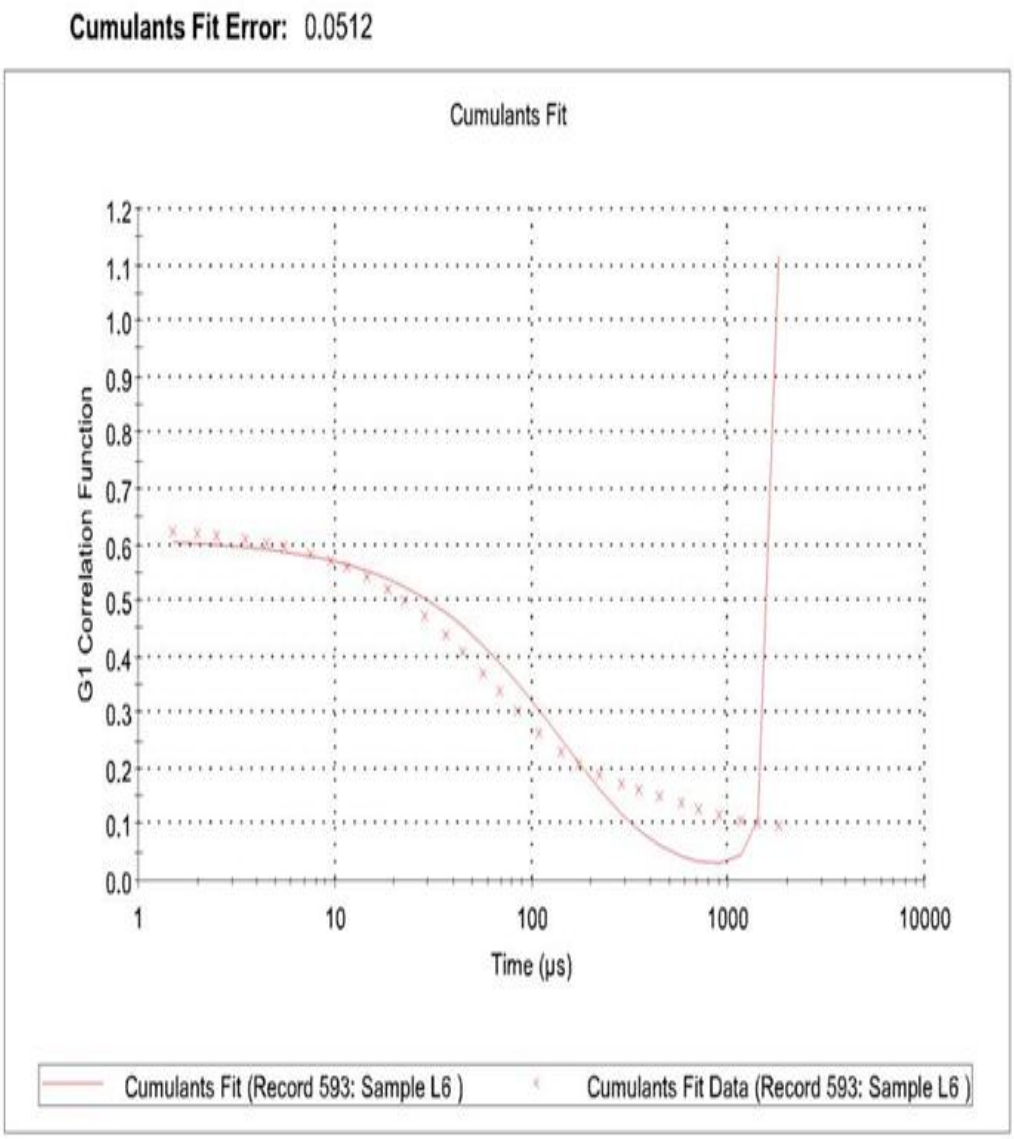

Figure 4.5: Cumulant fit coefficient

Figure 4.5: This report provides a quantitative measure of the fit quality used to derive the Z-Average and PDI, showing a Cumulants Fit Error of 0.0512. Since a reliable fit is typically below 0.02, this high value is the direct cause of the quality warning in Figure 4.4. The elevated error confirms that the sample exhibits a significant degree of polydispersity and/or aggregation, making the Z-Average value only an approximation of the average size.

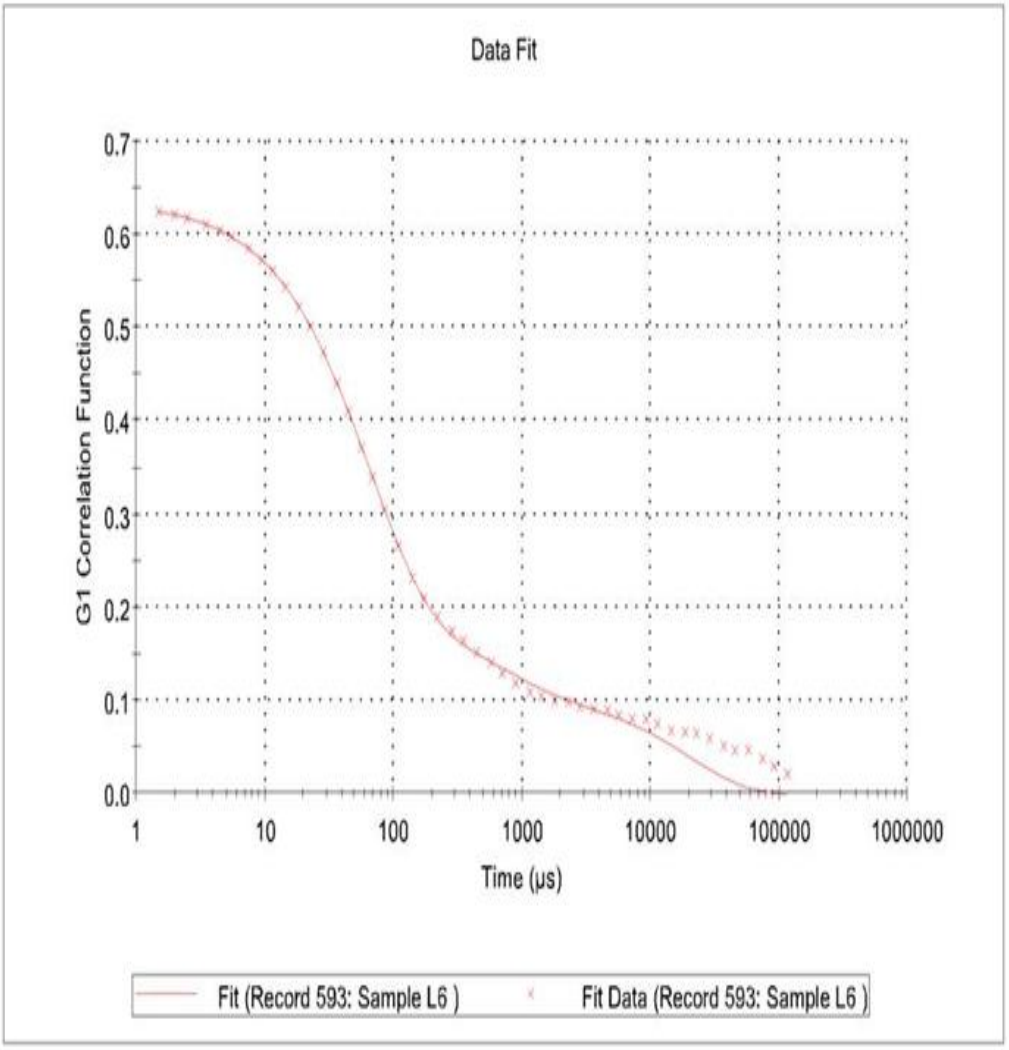

Figure 4.6: Distribution fit report

Figure 4.6: This figure shows the G1 Correlation Function (experimental data) overlaid with the corresponding computer-generated Fit Data (theoretical model). The close agreement between the experimental and fit curves, indicated by the near-perfect alignment of the data points and the dotted line, demonstrates that the distribution algorithm used to calculate the size distribution peaks was successful in modeling the underlying size populations within the heterogeneous sampleF

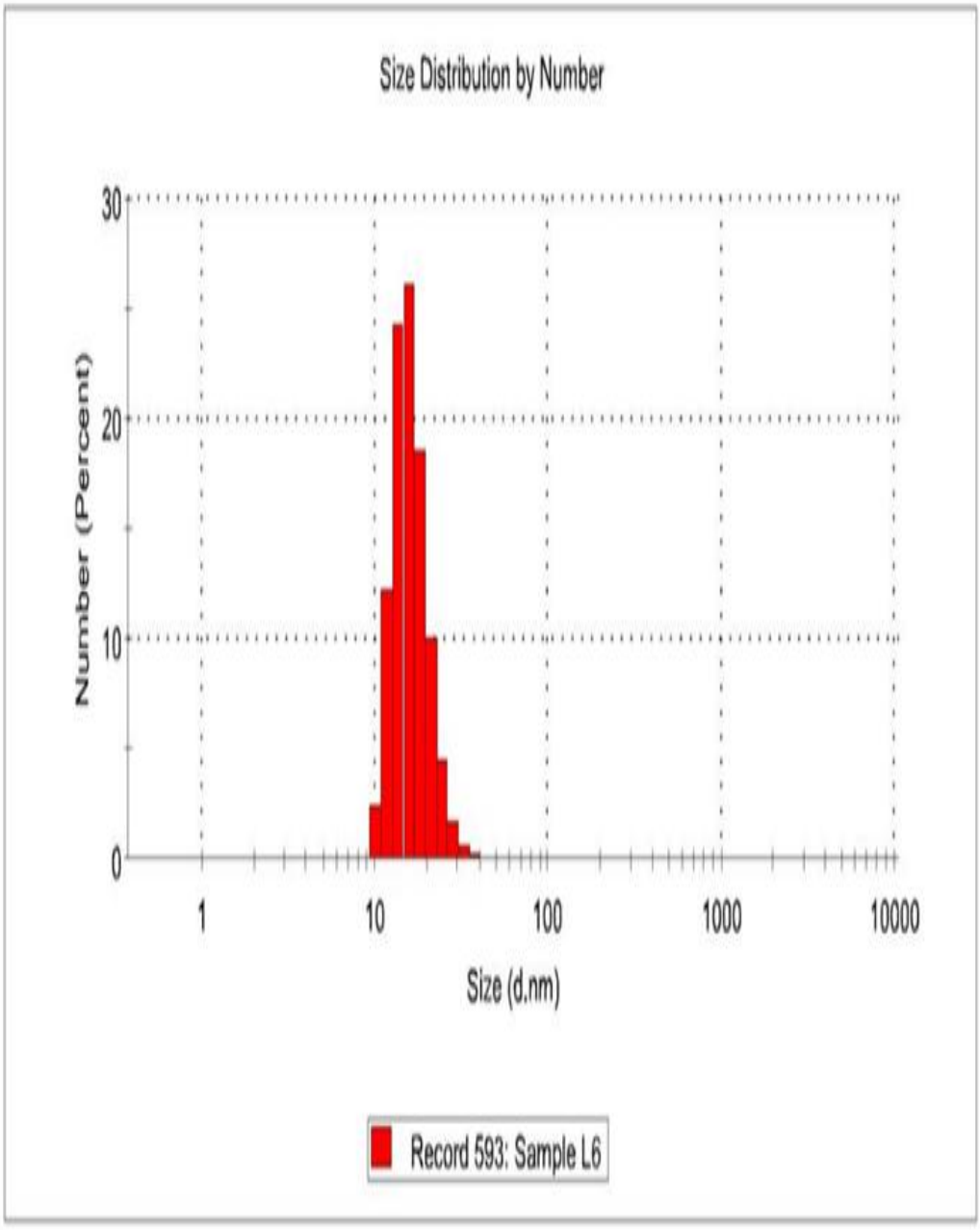

Figure 4.7: Size distribution by number

Figure 4.7: The Number Distribution report is highly sensitive to the smallest particles in the suspension, as it plots the actual count of particles in each size bin. This analysis clearly demonstrates that, by number, the entire synthesized product is overwhelmingly dominated by very small nanoparticles, with a single sharp peak at 16.25 nm accounting for 100.0% of the particle count. This figure is critical for confirming that the green synthesis route successfully generated a high concentration of nanoparticles in the desired size range.

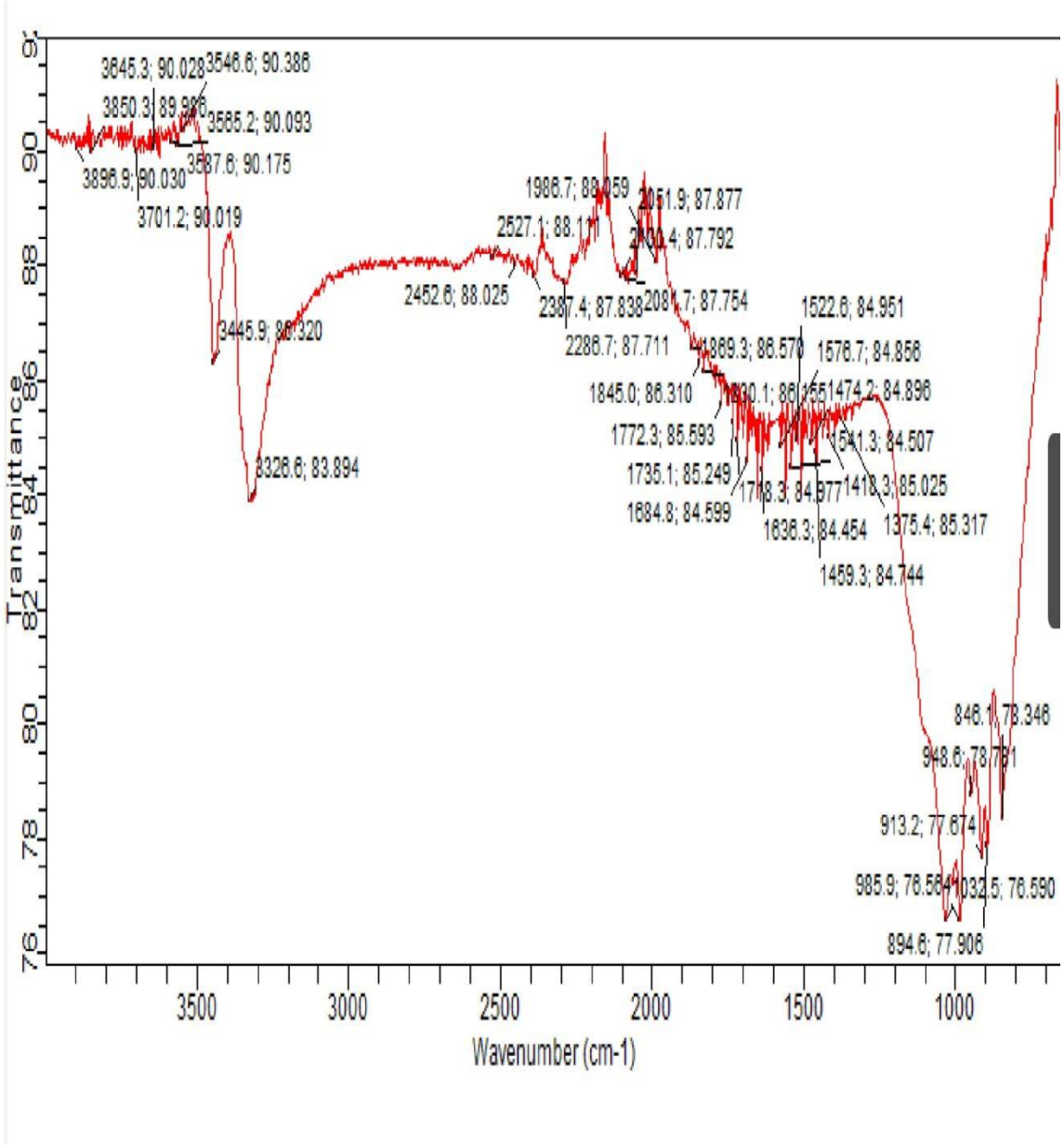

Figure 4.8: The Fourier-Transform Infrared (FTIR) spectrum provides crucial evidence of the organic functional groups present on the nanoparticle surface.

Figure 4.8: The FTIR spectrum confirms that molecules from the onion peel extract successfully attached to the surface of your copper chloride nanoparticles. The key evidence is the presence of specific chemical fingerprints in the graph. The very broad, strong dip around 3445.9 cm^{-1} is the signature of hydroxyl groups (O-H). These groups, found in natural compounds like phenols from the onion, act as the reducing agents needed to transform the copper precursor into nanoparticles. Additionally, the dips between 1600 and 1750cm^{-1} (e.g., 1772.3cm^{-1}, 1684.8 \$$cm^{-1}$) are from the C=O (carbonyl) groups of other organic molecules. These C=O and O-H compounds coat the surface of the nanoparticles like a protective shell, acting as capping or stabilizing agents to prevent them from clumping together (aggregation). In short, the spectrum proves the "green" nature of your synthesis by showing the plant compounds are integrated with the copper chloride NPs.

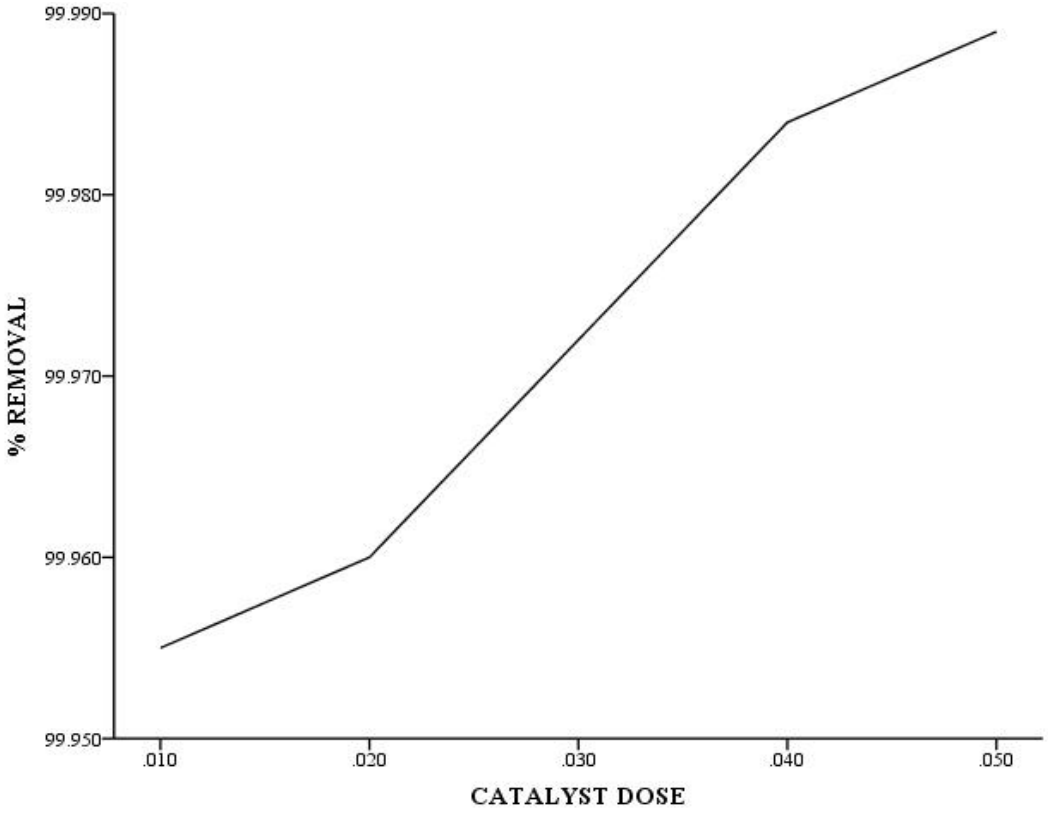

Figure 4.9: Effect of Catalyst on percentage removal

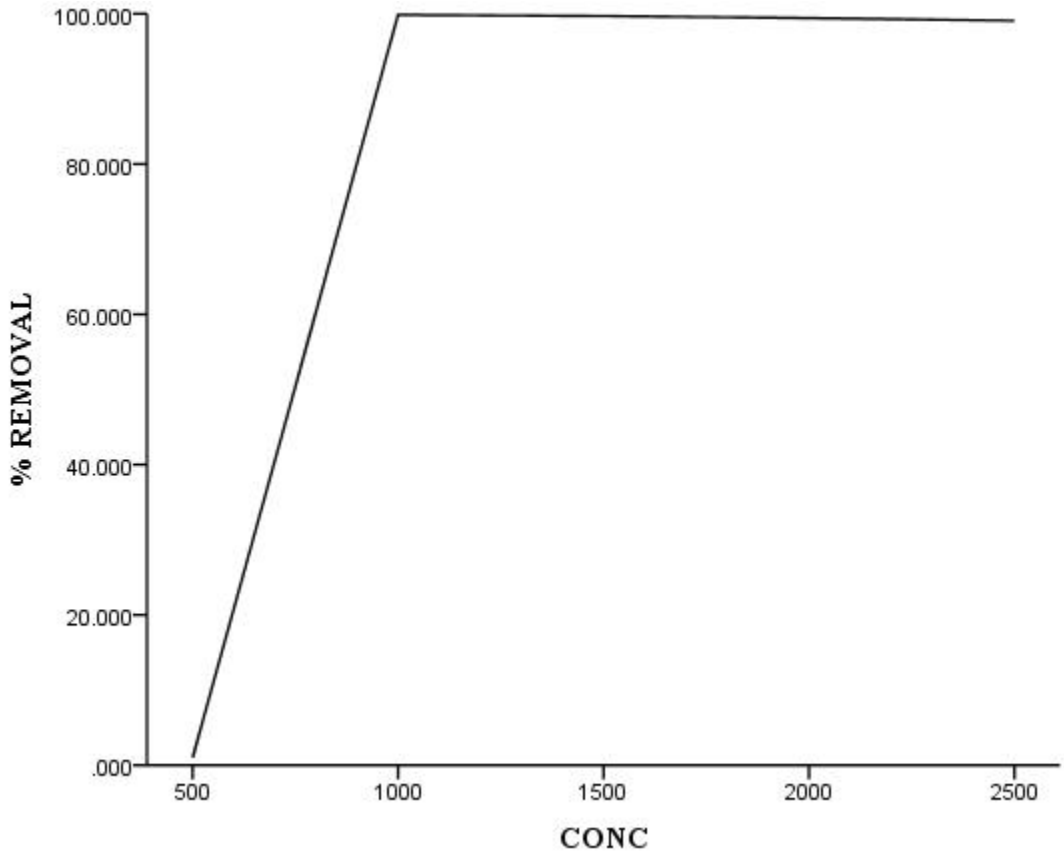

Figure 4.10: Effect of Concentration on percentage removal

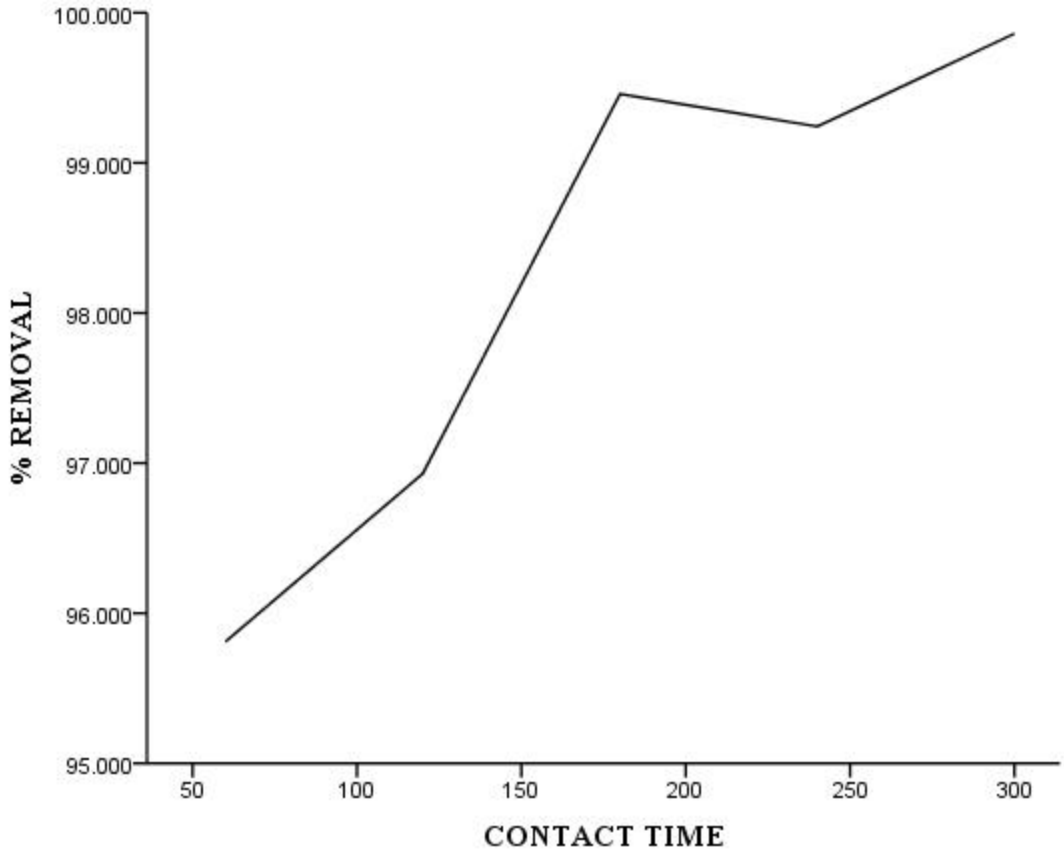

Figure 4.11: Effect of Contact time on percentage removal

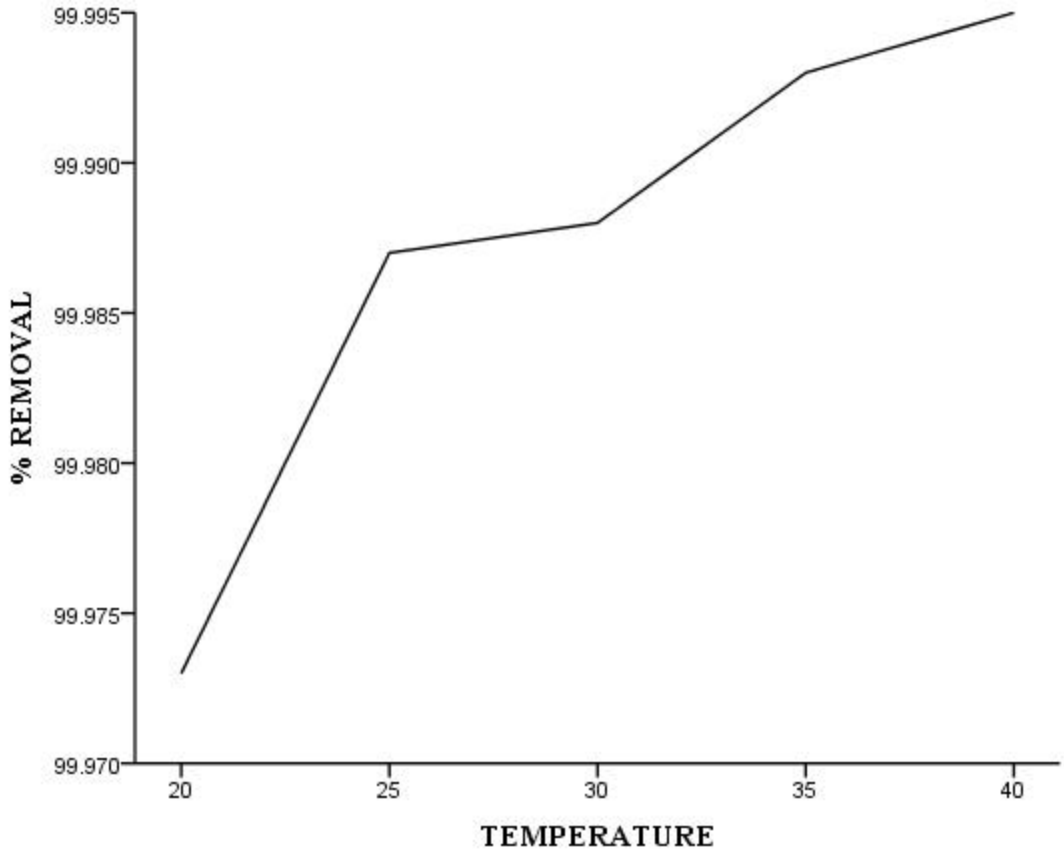

Figure 4.12: Effect of Temperature on percentage removal

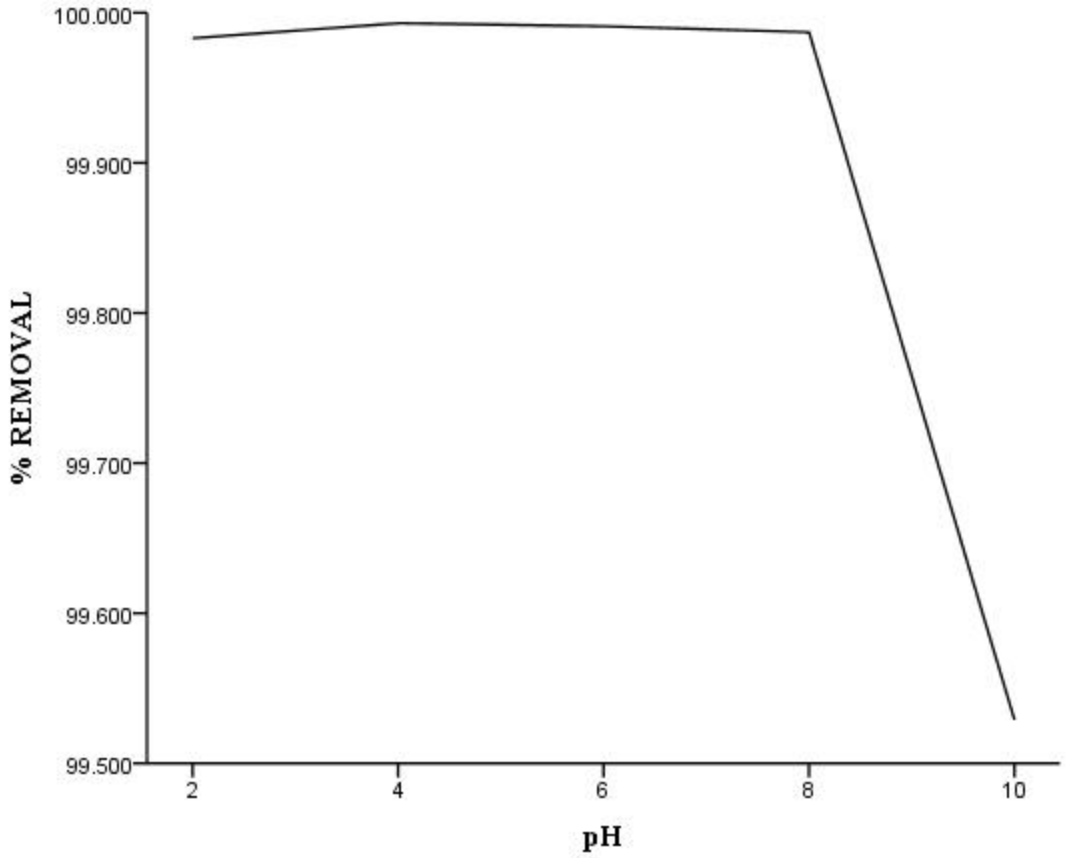

Figure 4.13: Effect of pH on percentage removal

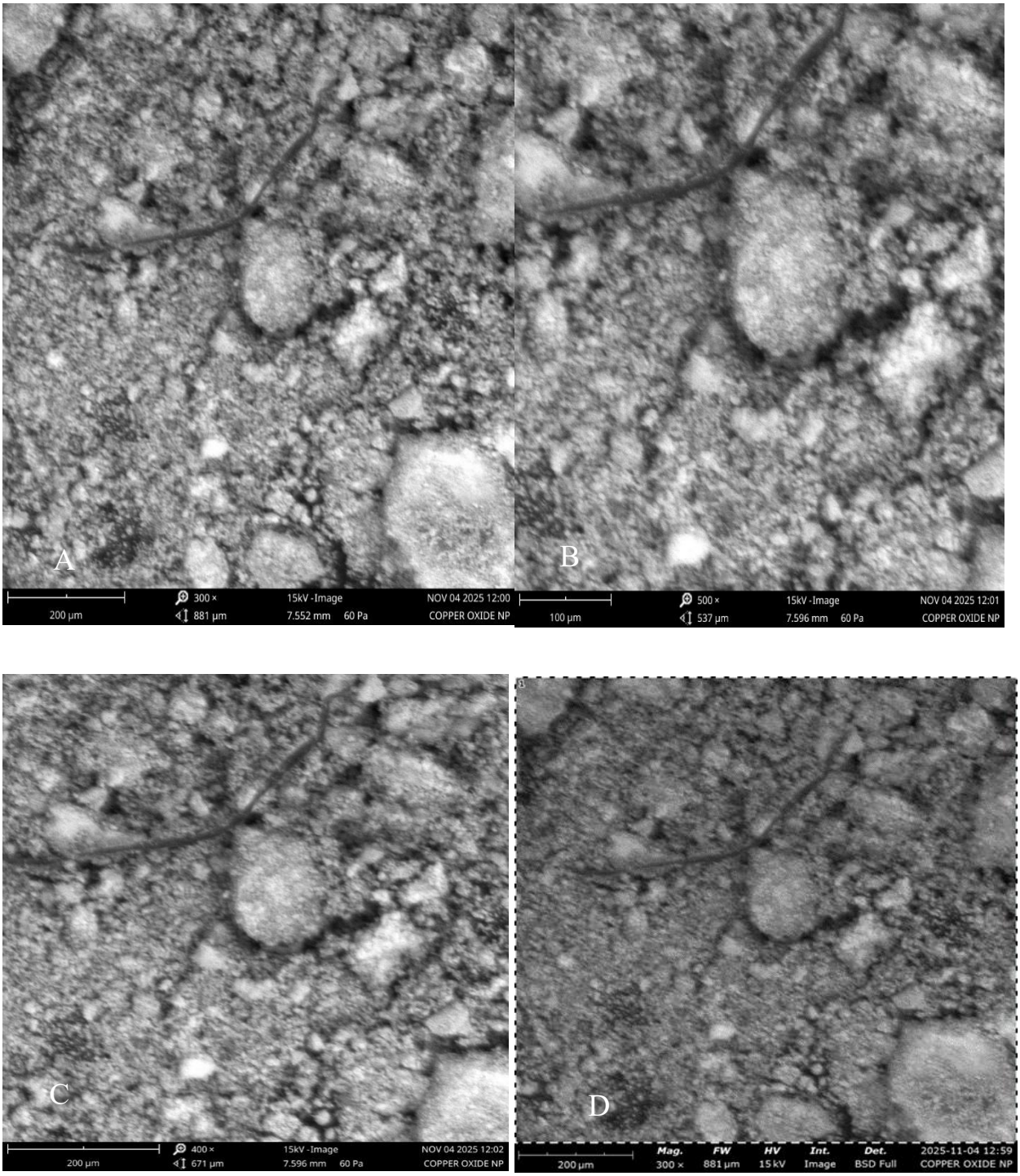

Figure 4.14: The biochar from pistachio shells loaded with $CuCl_2$ nanoparticles is shown in Figure 5e–h. The pictures demonstrate the deposition of ZnO particles by displaying nano-aggregates on the surface of the biochar. The contrast differences between bright and dark regions, where bright parts indicate high $CuCl_2$ concentrations, show that $CuCl_2$ usually occurs in spherical or flat nanostructures.

CHAPTER FIVE

DISCUSSION

The aim of this research was to synthesize copper chloride ($CuCl_2$) nanoparticles via a green route using onion peel extract and to evaluate their effectiveness in the photocatalytic degradation of crude oil in contaminated wastewater.

The successful green synthesis of $CuCl_2$ nanoparticles was first confirmed by the characterization results. Although there was some aggregation, the Dynamic Light Scattering (DLS) analysis, showed that the majority of the synthesized material, by number, consisted of nanoparticles with a primary size of 16.25 nm. This nanoscale dimension is important as it provides a high surface area to volume ratio, a fundamental property that enhances photocatalytic activity by offering more active sites for the adsorption and degradation of hydrocarbon pollutants. The presence of functional groups from the onion peel extract, confirmed by the FTIR spectrum specifically the broad O-H stretch at 3445.9 cm^{-1} and the C=O stretches between 1600 and 1750 cm^{-1} validates the role of the extract as both a reducing and a capping agent. The phytochemicals, such as flavonoids and phenolic compounds, are known and have been reported to facilitate the reduction of metal ions and stabilize the resulting nanoparticles, preventing excessive agglomeration and ensuring colloidal stability, which is a well researched advantage of plant-mediated synthesis (Ishak *et al.*, 2019; Singh *et al.*, 2018).

The analysis of the effect of catalyst dose revealed a trend in heterogeneous photocatalysis. It is anticipated that the degradation efficiency of Total Petroleum Hydrocarbons (TPH) will increase with an increasing dose of $CuCl_2$ nanoparticles up to an optimal point, after which a plateau or

decline will be observed. The initial increase is directly attributable to the greater availability of active sites on the nanoparticle surfaces. As more catalyst is introduced, a larger number of photons from the solar irradiation can be absorbed, generating more electron-hole pairs (e−*e*−/h+*h*+). These charge carriers are the primary agents for producing reactive oxygen species (ROS) like hydroxyl radicals (•OH) and superoxide anions ($\bullet O_2^-$), which are responsible for the oxidative breakdown of complex hydrocarbon chains into simpler, less harmful molecules like CO_2 and H_2O. However, beyond the optimal dose, the suspension becomes turbid, scattering and shielding the light from penetrating the solution, thereby reducing the photoactivation of a significant portion of the catalyst. This phenomenon of "light shielding" is a common limitation and has been observed in other studies, including that of Saien and Nejati (2007), who reported an optimal TiO_2 concentration of 100 mg L^{-1} for refinery wastewater treatment. Furthermore, high catalyst loadings can promote agglomeration, as hinted at in the DLS data, which reduces the effective surface area and accessibility of active sites.

The effect of solution pH was found to be a vital factor, with the highest photocatalytic efficiency in the acidic pH range. This can be rationalized by considering the surface charge of the $CuCl_2$ nanoparticles, which is governed by its point of zero charge (PZC). For most metal oxides, including copper-based nanoparticles, the surface is positively charged at a pH below the PZC. Since crude oil hydrocarbons are predominantly non-polar or weakly polar, an acidic environment (pH < PZC) creates a more favourable condition for the adsorption of these organic molecules onto the positively charged catalyst surface through electrostatic interactions. The effective transfer of photogenerated holes and ROS to the pollutant, which results in increased deterioration, depends on this close contact. On the other hand, the catalyst surface becomes negatively charged at neutral or basic pH, which may result in an electrostatic repulsion that

prevents oil components from adhering and slows down the pace of breakdown. This result is consistent with the work of Saien and Nejati (2007), who used TiO_2 to remove the most COD from wastewater from petroleum refineries at pH 3 and attributed this to the catalyst's surface charge characteristics.

A positive correlation between reaction temperature and degradation rate is expected within a moderate range. The effect of temperature on the photocatalytic process showed a positive correlation with degradation rate within a moderate range. Increased temperature enhances molecular kinetic energy, leading to more frequent collisions between pollutants and active sites, improved mass transfer, and facilitated desorption of degradation products. However, excessively high temperatures can accelerate the recombination of electron-hole pairs, competing with the redox reactions and reducing overall photocatalytic efficiency. The observed result aligns with conventional photocatalytic behavior, where an optimal temperature balances enhanced reaction kinetics with minimized charge carrier recombination. This complex interplay explains why an optimal temperature is often observed, as noted in the literature where a temperature of 318 K (45℃) was found to be optimal for TiO_2, balancing enhanced kinetics with the mitigation of charge carrier recombination.

The effect of initial pollutant concentration demonstrated that degradation efficiency decreases as the concentration of crude oil increases. At lower concentrations (e.g., 200-400 ppm), the ratio of catalyst active sites to hydrocarbon molecules is high, allowing for efficient degradation under a fixed light intensity and catalyst dose. However, at higher concentrations (e.g., 800-1000 ppm), the fixed number of active sites and the constant flux of photons become insufficient to degrade the large quantity of pollutant molecules. Furthermore, high turbidity caused by the oil itself can limit light penetration, reducing the photon availability for exciting the catalyst. This inverse

relationship between initial concentration and removal efficiency is a common feature in photocatalytic systems.

With longer irradiation times, contact time demonstrated a steady rise in TPH degradation. The degradation efficiency improved with increased contact time, as longer irradiation durations allow for sustained photon absorption and continuous generation of ROS, enabling the progressive breakdown of refractory hydrocarbon components. This time-dependent enhancement is typical in photocatalytic processes, where degradation rates are often rapid initially and then slow as more recalcitrant compounds remain.

CONCLUSION

The green-synthesised $CuCl_2$ nanoparticles' photocatalytic activity depends on a number of intricately interconnected factors. The results of this investigation are consistent with the larger body of research on photocatalysis for wastewater treatment. The proven effectiveness of onion peel-stabilized $CuCl_2$ nanoparticles under ideal catalyst dose, pH, temperature, and contact time settings makes this green technology a very viable, sustainable, and affordable option for cleaning up crude oil-contaminated water, especially in Nigeria's environmentally delicate Niger Delta.

REFERENCES

Agbe, H., Nyankson, E., Raza, N., Dodoo-Arhin, D., Chauhan, A., Osei, G., Kumar, V. and Kim, K. H. (2019). Recent advances in photoinduced catalysis for water splitting and environmental applications. *Journal of Industrial and Engineering Chemistry*, **72**: 31-49.

Akhtar, M. S., Panwar, J. and Yun, Y. S. (2013). Biogenic synthesis of metallic nanoparticles by plant extracts. *ACS Sustainable Chemistry and Engineering*, **1**(6): 591-602.

Aminuzzaman, M., Kei, L. M. and Liang, W. H. (2017), April. Green synthesis of copper oxide (CuO) nanoparticles using banana peel extract and their photocatalytic activities. In *AIP Conference Proceedings* (Vol. 1828, No. 1, p. 020016). AIP Publishing LLC.

Asghar, M. A., Zahir, E., Shahid, S. M., Khan, M. N., Asghar, M. A., Iqbal, J. and Walker, G. (2018). Iron, copper and silver nanoparticles: Green synthesis using green and black tea leaves extracts and evaluation of antibacterial, antifungal and aflatoxin B1 adsorption activity. *Lwt*, **90**: 98-107.

Bonatto, C. C. and Silva, L. P. (2014). Higher temperatures speed up the growth and control the size and optoelectrical properties of silver nanoparticles greenly synthesized by cashew nutshells. *Industrial Crops and Products*, **58**: 46-54.

Chong, M. N., Jin, B., Chow, C. W. and Saint, C. (2010). Recent developments in photocatalytic water treatment technology: a review. *Water Research*, **44**(10): 997-3027.

Chung, I. M., Abdul Rahuman, A., Marimuthu, S., Vishnu Kirthi, A., Anbarasan, K., Padmini, P. and Rajakumar, G. (2017). Green synthesis of copper nanoparticles using Eclipta prostrata leaves extract and their antioxidant and cytotoxic activities. *Experimental and Therapeutic Medicine*, **14**(1): 18-24.

Coto, M., Divitini, G., Dey, A., Krishnamurthy, S., Ullah, N., Ducati, C. and Kumar, R. V. (2017). Tuning the properties of a black TiO2-Ag visible light photocatalyst produced by a rapid one-pot chemical reduction. *Materials Today Chemistry*, **4**: 142-149.

Delma, M. T., Vijila, B. and Rajan, M. J. (2016). Green synthesis of copper and lead nanoparticles using ZingiberOfficinale stemextract. *International Journal of Scientific and Research Publications*, **6**(11): 134-137.

Dodoo-Arhin, D., Buabeng, F. P., Mwabora, J. M., Amaniampong, P. N., Agbe, H., Nyankson, E., Obada, D. O. and Asiedu, N. Y. (2018). The effect of titanium dioxide synthesis technique and its photocatalytic degradation of organic dye pollutants. *Heliyon*, **4**(7).

Dodoo-Arhin, D., Buabeng, F. P., Mwabora, J. M., Amaniampong, P. N., Agbe, H., Nyankson, E., Obada, D. O. and Asiedu, N. Y. (2018). The effect of titanium dioxide synthesis technique and its photocatalytic degradation of organic dye pollutants. *Heliyon*, **4**(7).

Eastman, J. A., Choi, S. U. S., Li, S., Yu, W. and Thompson, L. J. (2001). Anomalously increased effective thermal conductivities of ethylene glycol-based nanofluids containing copper nanoparticles. *Applied Physics Letters*, **78**(6): 718-720.

Efavi, J. K., Nyankson, E., Yaya, A. and Agyei-Tuffour, B. (2017). Effect of magnesium and sodium salts on the interfacial characteristics of soybean lecithin dispersants. *Industrial and Engineering Chemistry Research*, **56**(44): 12608-12620.

Efavi, J. K., Nyankson, E., Yaya, A. and Agyei-Tuffour, B. (2017). Effect of magnesium and sodium salts on the interfacial characteristics of soybean lecithin dispersants. *Industrial and Engineering Chemistry Research*, **56**(44): 12608-12620.

El-Sayyad, G. S., Elfadil, D., Mosleh, M. A., Hasanien, Y. A., Mostafa, A., Abdelkader, R. S., Refaey, N., Elkafoury, E. M., Eshaq, G., Abdelrahman, E. A. and Malash, M. N. (2024). Eco-friendly strategies for biological synthesis of green nanoparticles with promising applications. *BioNanoScience*, **14**(3): 3617-3659.

Etkin, D. S. (2001), March. Analysis of oil spill trends in the United States and worldwide. In *International oil spill conference* (Vol. 2001, No. 2, pp. 1291-1300). American Petroleum Institute.

Fàbrega, C., Andreu, T., Cabot, A. and Morante, J. R. (2010). Location and catalytic role of iron species in TiO2: Fe photocatalysts: An EPR study. *Journal of Photochemistry and Photobiology A: Chemistry*, **211**(2-3): 170-175.

Fujishima, A. and Zhang, X. (2006). Titanium dioxide photocatalysis: present situation and future approaches. *Comptes Rendus. Chimie*, **9**(5-6): 750-760.

Fujishima, A., Zhang, X. and Tryk, D. A. (2007). Heterogeneous photocatalysis: from water photolysis to applications in environmental cleanup. *International Journal of Hydrogen Energy*, **32**(14): 2664-2672.

Gopinath, M., Subbaiya, R., Selvam, M. M. and Suresh, D. (2014). Synthesis of copper nanoparticles from Nerium oleander leaf aqueous extract and its antibacterial activity. *International Journal of Current Microbiology and Applied Science*, **3**(9): 814-818.

Guduru, R. K., Murty, K. L., Youssef, K. M., Scattergood, R. O. and Koch, C. C. (2007). Mechanical behavior of nanocrystalline copper. *Materials Science and Engineering: A*, **463**(1-2): 14-21.

Huang, F., Yan, A. and Zhao, H. (2016). Influences of Doping on Photocatalytic Properties of TiO_2 Photocatalyst. *Semiconductor Photocatalysis: Materials, Mechanisms and Applications*, **40**: 31.

Iavicoli, I., Leso, V., Ricciardi, W., Hodson, L. L. and Hoover, M. D. (2014). Opportunities and challenges of nanotechnology in the green economy. *Environmental Health*, **13**(1): 78.

Ishak, N. M., Kamarudin, S. K. and Timmiati, S. N. (2019). Green synthesis of metal and metal oxide nanoparticles via plant extracts: an overview. *Materials Research Express*, **6**(11): 112004.

Issaabadi, Z., Nasrollahzadeh, M. and Sajadi, S. M. (2017). Green synthesis of the copper nanoparticles supported on bentonite and investigation of its catalytic activity. *Journal of Cleaner Production*, **142**: 3584-3591.

Khani, R., Roostaei, B., Bagherzade, G. and Moudi, M. (2018). Green synthesis of copper nanoparticles by fruit extract of *Ziziphus spina-christi* (L.) Willd.: Application for adsorption of triphenylmethane dye and antibacterial assay. *Journal of Molecular Liquids*, **255**: 541-549.

Kharisov, B. I., Dias, H. R., Kharissova, O. V., Jiménez-Pérez, V. M., Pérez, B. O. and Flores, B. M. (2012). Iron-containing nanomaterials: synthesis, properties, and environmental applications. *Rsc Advances*, **2**(25): 9325-9358.

Kulkarni, V. D. and Kulkarni, P. S. (2013). Green synthesis of copper nanoparticles using Ocimum sanctum leaf extract. *International Journal of Chemical Studies*, **1**(3): 1-4.

Kumar, P. V., Shameem, U., Kollu, P., Kalyani, R. L. and Pammi, S. V. N. (2015). Green synthesis of copper oxide nanoparticles using Aloe vera leaf extract and its antibacterial activity against fish bacterial pathogens. *BioNanoScience*, **5**(3): 135-139.

Lu, B., Ma, N., Wang, Y., Qiu, Y., Hu, H., Zhao, J., Liang, D., Xu, S., Li, X., Zhu, Z. and Cui, C., 2015. Visible-light-driven TiO2/Ag3PO4/GO heterostructure photocatalyst with dual-channel for photo-generated charges separation. *Journal of Alloys and Compounds*, **630**: 163-171.

Manjari, G., Saran, S., Arun, T., Rao, A. V. B. and Devipriya, S. P. (2017). Catalytic and recyclability properties of phytogenic copper oxide nanoparticles derived from Aglaia elaeagnoidea flower extract. *Journal of Saudi Chemical Society*, **21**(5): 610-618.

Meng, H., Wang, B., Liu, S., Jiang, R. and Long, H. (2013). Hydrothermal preparation, characterization and photocatalytic activity of TiO2/Fe–TiO2 composite catalysts. *Ceramics International*, **39**(5): 5785-5793.

Mittal, A. K., Chisti, Y. and Banerjee, U. C. (2013). Synthesis of metallic nanoparticles using plant extracts. *Biotechnology Advances*, **31**(2): 346-356.

Mondal, A. K., Mondal, S., Samanta, S. and Mallick, S. (2011). Synthesis of ecofriendly silver nanoparticle from plant latex used as an important taxonomic tool for phylogenetic interrelationship advances in bioresearch vol. 2. *Synthesis*, **31**: 33.

MubarakAli, D., Thajuddin, N., Jeganathan, K. and Gunasekaran, M. (2011). Plant extract mediated synthesis of silver and gold nanoparticles and its antibacterial activity against clinically isolated pathogens. *Colloids and Surfaces B: Biointerfaces*, **85**(2): 360-365.

Muthulakshmi, L., Rajini, N., Nellaiah, H., Kathiresan, T., Jawaid, M. and Rajulu, A. V. (2017). Preparation and properties of cellulose nanocomposite films with in situ generated copper nanoparticles using Terminalia catappa leaf extract. *International Journal of Biological Macromolecules*, **95**: 1064-1071.

Nagajyothi, P. C., Muthuraman, P., Sreekanth, T. V. M., Kim, D. H. and Shim, J. (2017). Green synthesis: in-vitro anticancer activity of copper oxide nanoparticles against human cervical carcinoma cells. *Arabian Journal of Chemistry*, **10**(2): 215-225.

Nagar, N. and Devra, V. (2018). Green synthesis and characterization of copper nanoparticles using Azadirachta indica leaves. *Materials Chemistry and Physics*, **213**: 44-51.

Narasaiah, P., Mandal, B. K. and Sarada, N. C. (2017). November. Biosynthesis of copper oxide nanoparticles from Drypetes sepiaria leaf extract and their catalytic activity to dye degradation. In *IOP conference series: Materials Science and Engineering* (Vol. 263, No. 2, p. 022012). IOP Publishing.

Narayanan, K. B. and Sakthivel, N. (2011). Green synthesis of biogenic metal nanoparticles by terrestrial and aquatic phototrophic and heterotrophic eukaryotes and biocompatible agents. *Advances in Colloid and Interface Science*, **169**(2): 59-79.

Nasiri, E. F., Kebria, D.Y. and Qaderi, F. (2018). An experimental study on the simultaneous phenol and chromium removal from water using titanium dioxide photocatalyst. *Civil Engineering Journal*, **4**(3): 585-593.

Nasrollahzadeh, M. and Sajadi, S. M. (2015). Green synthesis of copper nanoparticles using Ginkgo biloba L. leaf extract and their catalytic activity for the Huisgen [3+ 2] cycloaddition of azides and alkynes at room temperature. *Journal of Colloid and Interface Science*, **457**: 141-147.

Nasrollahzadeh, M., Momeni, S. S. and Sajadi, S. M. (2017). Green synthesis of copper nanoparticles using *Plantago asiatica* leaf extract and their application for the cyanation of aldehydes using K4Fe (CN) 6. *Journal of Colloid and Interface Science*, **506**: 471-477.

Nasrollahzadeh, M., Sajadi, S. M. and Rostami-Vartooni, A. (2015). Green synthesis of CuO nanoparticles by aqueous extract of Anthemis nobilis flowers and their catalytic activity for the A3 coupling reaction. *Journal of Colloid and Interface Science*, **459**: 183-188.

Nazar, N., Bibi, I., Kamal, S., Iqbal, M., Nouren, S., Jilani, K., Umair, M. and Ata, S. (2018). Cu nanoparticles synthesis using biological molecule of *P. granatum* seeds extract as

reducing and capping agent: Growth mechanism and photo-catalytic activity. *International Journal of Biological Macromolecules*, **106**: 1203-1210.

Nyankson, E., DeCuir, M. J. and Gupta, R. B. (2015). Soybean lecithin as a dispersant for crude oil spills. *ACS Sustainable Chemistry and Engineering*, **3**(5): 920-931.

Nyankson, E., Demir, M., Gonen, M. and Gupta, R. B. (2016). Interfacially active hydroxylated soybean lecithin dispersant for crude oil spill remediation. *ACS Sustainable Chemistry and Engineering*, **4**(4): 2056-2067.

Nyankson, E., Ober, C. A., DeCuir, M. J. and Gupta, R. B. (2014). Comparison of the effectiveness of solid and solubilized dioctyl sodium sulfosuccinate (DOSS) on oil dispersion using the baffled flask test, for crude oil spill applications. *Industrial and Engineering Chemistry Research*, **53**(29): 11862-11872.

Nyankson, E., Rodene, D. and Gupta, R. B. (2016). Advancements in crude oil spill remediation research after the Deepwater Horizon oil spill. *Water, Air, and Soil Pollution*, **227**(1): 29.

Ohanmu, E. O., Bako, S. P., Ohanmu, E. and Ohanmu, O. O. (2019). Environmental implications, properties and attributes of crude oil in the oil-producing states of Nigeria. *Ecologia*, **9**(1): 1-9.

Owoseni, O., Nyankson, E., Zhang, Y., Adams, S. J., He, J., McPherson, G. L., Bose, A., Gupta, R. B. and John, V. T. (2014). Release of surfactant cargo from interfacially-active halloysite clay nanotubes for oil spill remediation. *Langmuir*, **30**(45): 13533-13541.

Park, Y., Hong, Y. N., Weyers, A., Kim, Y. S. and Linhardt, R. J. (2011). Polysaccharides and phytochemicals: a natural reservoir for the green synthesis of gold and silver nanoparticles. *IET Nanobiotechnology*, **5**(3): 69-78.

Plata, D. L., Sharpless, C. M. and Reddy, C. M. (2008). Photochemical degradation of polycyclic aromatic hydrocarbons in oil films. *Environmental Science and Technology*, **42**(7): 2432-2438.

Prasad, K. S., Patra, A., Shruthi, G. and Chandan, S. (2017). Aqueous extract of Saraca indica leaves in the synthesis of copper oxide nanoparticles: finding a way towards going green. *Journal of Nanotechnology*, **2017**(1): 7502610.

Quester, K., Avalos-Borja, M., Vilchis-Nestor, A. R., Camacho-López, M. A. and Castro-Longoria, E. (2013). SERS properties of different sized and shaped gold nanoparticles biosynthesized under different environmental conditions by Neurospora crassa extract. *PloS one*, **8**(10): e77486.

Rajesh, K. M., Ajitha, B., Reddy, Y. A. K., Suneetha, Y. and Reddy, P. S. (2018). Assisted green synthesis of copper nanoparticles using Syzygium aromaticum bud extract: Physical, optical and antimicrobial properties. *Optik*, **154**: 593-600.

Ravindra, S., Mohan, Y. M., Reddy, N. N. and Raju, K. M. (2010). Fabrication of antibacterial cotton fibres loaded with silver nanoparticles via "Green Approach". *Colloids and surfaces A: Physicochemical and Engineering Aspects*, **367**(1-3): 31-40.

Salem, H. H. and Ghouniem, N. T. (2022). The Impact of Oil Spills on the Environment and Surrounding Communities: Case of Spain and Brazil. *MSA-Management Sciences Journal*, **1**(1): 1-19.

Sam, K., Coulon, F. and Prpich, G. (2016). Working towards an integrated land contamination management framework for Nigeria. *Science of the Total Environment*, **571**: 916-925.

Santos, R. D. S., Faria, G. A., Giles, C., Leite, C. A., Barbosa, H. D. S., Arruda, M. A. and Longo, C. (2012). Iron insertion and hematite segregation on Fe-doped TiO2 nanoparticles obtained from sol–gel and hydrothermal methods. *ACS Applied Materials and Interfaces*, **4**(10): 5555-5561.

Sharma, P., Pant, S., Poonia, P., Kumari, S., Dave, V. and Sharma, S. (2018). Green synthesis of colloidal copper nanoparticles capped with Tinospora cordifolia and its application in catalytic degradation in textile dye: an ecologically sound approach. *Journal of Inorganic and Organometallic Polymers and Materials*, **28**(6): 2463-2472.

Sharmila, G., Pradeep, R. S., Sandiya, K., Santhiya, S., Muthukumaran, C., Jeyanthi, J., Kumar, N. M. and Thirumarimurugan, M. (2018). Biogenic synthesis of CuO nanoparticles using *Bauhinia tomentosa* leaves extract: Characterization and its antibacterial application. *Journal of Molecular Structure*, **1165**: 288-292.

Shayegan Mehr, E., Sorbiun, M., Ramazani, A. and Taghavi Fardood, S. (2018). Plant-mediated synthesis of zinc oxide and copper oxide nanoparticles by using ferulago angulata (schlecht) boiss extract and comparison of their photocatalytic degradation of Rhodamine B (RhB) under visible light irradiation. *Journal of Materials Science: Materials in Electronics*, **29**(2): 1333-1340.

Shende, S., Ingle, A. P., Gade, A. and Rai, M. (2015). Green synthesis of copper nanoparticles by *Citrus medica* Linn (Idilimbu) juice and its antimicrobial activity. *World Journal of Microbiology and Biotechnology*, **31**(6): 865-873.

Singh, J., Dutta, T., Kim, K. H., Rawat, M., Samddar, P. and Kumar, P. (2018). 'Green'synthesis of metals and their oxide nanoparticles: applications for environmental remediation. *Journal of Nanobiotechnology*, **16**(1): 84.

Sivaraj, R., Rahman, P. K., Rajiv, P., Salam, H. A. and Venckatesh, R. (2014). Biogenic copper oxide nanoparticles synthesis using Tabernaemontana divaricate leaf extract and its antibacterial activity against urinary tract pathogen. *Spectrochimica Acta Part A: Molecular and Biomolecular Spectroscopy*, **133**: 178-181.

Sorbiun, M., Shayegan Mehr, E., Ramazani, A. and Taghavi Fardood, S. (2018). Green synthesis of zinc oxide and copper oxide nanoparticles using aqueous extract of oak fruit hull (jaft) and comparing their photocatalytic degradation of basic violet 3. *International Journal of Environmental Research*, **12**(1): 29-37.

Tan, Y. N., Lee, J. Y. and Wang, D. I. (2010). Uncovering the design rules for peptide synthesis of metal nanoparticles. *Journal of the American Chemical Society*, **132**(16): 5677-5686.

Thakkar, K. N., Mhatre, S. S. and Parikh, R. Y. (2010). Biological synthesis of metallic nanoparticles. *Nanomedicine: Nanotechnology, Biology and Medicine*, **6**(2): 257-262.

Thakur, S., Sharma, S., Thakur, S. and Rai, R. (2018). Green synthesis of copper nano-particles using Asparagus adscendens roxb. Root and leaf extract and their antimicrobial activities. *International Journal Current Microbiology and Applied Science*, **7**(4): 683-694.

Umar, H. A., Khanan, M. A., Ogbonnaya, C., Shiru, M. S., Ahmad, A. and Baba, A. I. (2021). Environmental and socioeconomic impacts of pipeline transport interdiction in Niger Delta, Nigeria. *Heliyon*, **7**(5).

Varma, R. S. (2012). Greener approach to nanomaterials and their sustainable applications. *Current Opinion in Chemical Engineering*, **1**(2): 123-128.

Vishveshvar, K., Aravind Krishnan, M. V., Haribabu, K. and Vishnuprasad, S. (2018). Green synthesis of copper oxide nanoparticles using *Ixiro coccinea* plant leaves and its characterization. *BioNanoScience*, **8**(2): 554-558.

Wardak, A., Gorman, M. E., Swami, N. and Rejeski, D. (2007). Environmental Regulation of Nanotechnology and the TSCA. *IEEE Technology and Society Magazine*, **26**(2): 48-56.

Xia, T., Li, N. and Nel, A. E. (2009). Potential health impact of nanoparticles. *Annual Review of Public Health*, **30**(1): 137-150.

Xing, M., Zhang, J., Chen, F. and Tian, B. (2011). An economic method to prepare vacuum activated photocatalysts with high photo-activities and photosensitivities. *Chemical Communications*, **47**(17): 4947-4949.

Yehia, M., Labib, S. and Ismail, S. M. (2014). Structural and magnetic properties of nano-NiFe2O4 prepared using green nanotechnology. *Physica B: Condensed Matter*, **446**: 49-54.

Zabbey, N., Sam, K. and Onyebuchi, A. T. (2017). Remediation of contaminated lands in the Niger Delta, Nigeria: Prospects and challenges. *Science of the Total Environment*, **586**: 952-965.

Ziervogel, K., McKay, L., Rhodes, B., Osburn, C. L., Dickson-Brown, J., Arnosti, C. and Teske, A. (2012). Microbial activities and dissolved organic matter dynamics in oil-contaminated surface seawater from the Deepwater Horizon oil spill site. *PloS one*, **7**(4): e34816.